Physico-mechanical Properties of Treated Oil Palm Broom Fibres for Cementitious Composites

Emmanuel Owoichoechi Momoh[1] Adelaja Israel Osofero[2] Oleksandr Menshykov[3]

School of Engineering, University of Aberdeen, King's College, Aberdeen, AB24 3UE, United Kingdom, r01eom18@abdn.ac.uk[1]

School of Engineering, University of Aberdeen, King's College, Aberdeen, AB24 3UE, United Kingdom, aiosofero@abdn.ac.uk[2]

School of Engineering, University of Aberdeen, King's College, Aberdeen, AB24 3UE, United Kingdom. o.menshykov@abdn.ac.uk[3]

Abstract

The use of natural fibres such as oil palm broom fibres (OPBF) for reinforcing cementitious composites though reported to be beneficial from economic and environmental standpoints have generated durability concerns that have caused investigations into possible fibre treatments. In this study, three (3) types of treatments were carried out on OPBF. These include alkalisation, silanization and hot-water treatments. For alkalisation, OPBF were treated with solutions of 2%, 4%, 6% and 10% sodium hydroxide each for 30, 60, 120, 240, 480, 1440 and 2880 minutes. For silanization, OPBF were treated with solutions of 1% and 3% triethoxyvinylsilane each for 60, 120, 240, 480, 1440 and 2880 minutes. For hot-water treatment, OPBF were treated with water at 100^{0}C for 15, 30, 60 and 120 minutes. Effects of treatments on the fibres were analysed through tensile strength, x-ray diffraction, electron microscopy and water absorption tests. Results show improvements in tensile strength and modulus of elasticity of 60% and 65% respectively. While average reduction in water absorption of 4% was recorded for silanization, an increase of 40% and 9% were recorded for alkalisation and hot-water treatment respectively. The changes in the physical and mechanical properties of treated OPBF are attributed to the elimination of impurities, lignin and wax, reduction of microfibrillar angle, alteration of fibre surface and improvement in fibre crystallinity. The reported pre-treatments could enhance the durability of composites incorporating OPBF as reinforcement.

KEYWORDS: Alkalisation; Cement; Characterisation; Composites; Mechanical properties; Natural fibres; Polymer; Silane treatment.

Corresponding Author: Osofero, Adelaja Israel[2]

School of Engineering, University of Aberdeen, King's College, Aberdeen, United Kingdom

aiosofero@abdn.ac.uk

Introduction

Recent concerns on global environmental wellness and sustainability have favoured the use of natural materials as an alternative to synthetic ones in both cementitious and polymeric composites. Advantages such as low carbon footprint, non-toxicity to the ecosystem, light-weightiness, availability, low-cost, toughness, biodegradability, thermal insulation, impressive mechanical properties and high-recyclability associated with the use of plant fibres have attracted research interest in recent years. Plant fibres are referred to as lignocellulosic fibres since they consist mainly of cellulose, hemicellulose, lignin, pectin and waxy compounds with cellulose considered as the main structural component (Kabir et al. 2012). The oil palm tree (*Elaeis guineensis*), an abundant source of vegetable fibre, is a monocotyledonous plant available in 42 countries of the world spread across Asia, Africa and South America and is one of the world's leading food crops (Momoh and Osofero 2020). It is grown mainly for the production of cooking oil, but the by-product of the oil extraction process generates huge masses of waste biomass. These wastes include oil palm shells, empty fruit bunch fibres (EFBF), oil palm mesocarp fibres (OPMF), trunk fibres (OPTF), frond fibres (OPFF) and broom fibres (OPBF). OPBF are the ribs of the leaflets of the oil palm tree and is also popular for its use as broom bristles. An illustration of OPBF from oil palm fronds can be found in Momoh and Osofero (2019).

Generally, oil palm fibres do not rot easily and are indiscriminately discarded in the environment or used as cooking fuel in developing countries (Ismail and Yaacob 2011; Sreekala and Thomas 2002). Similar to other natural lignocellulosic fibres, there is the problem of variations in physical and mechanical properties even among fibres from the same oil palm species (Fortea-Verdejo et al. 2017) together with durability concerns when the fibres are used in alkaline environment (Ardanuy et al. 2015; Claramunt et al. 2016). Aside fibre impurities in form of wax, fatty compounds and globular protrusions (referred to as *tyloses*) (Sreekala et al. 1997; Izani et al. 2013), hemicellulose, lignin and pectin are easily dissolved at the interfacial zone between fibre and matrix and are responsible for poor bonding with matrices (Pacheco-Torgal and Jalali 2010; Zhou et al. 2016). The type of cellulose and its corresponding cell geometry have also been reported as factors affecting the mechanical properties of vegetable fibres and their interaction with matrices (Kabir et al. 2012). Furthermore, the hydrophilicity of natural fibres makes them

dimensionally unstable. During moisture absorption, fibre sizes increase, hence creating internal stresses in the matrix. Conversely, the fibres shrink and are debonded from the matrix under dry conditions (Sreekala and Thomas 2002; Muñoz and García-Manrique 2015). This causes a reduction in the strength of the composite. Treatment of natural fibres is therefore carried out to enhance fibre strength, eliminate unwanted compounds, reduce water absorption and enhance bonding with matrices. Such treatments include, but not limited to, alkalisation (Sreekala et al. 1997; Nishiyamo and Okano 1998; Machaka et al. 2014), salinization (Sreekala et al. 1997; Bilba and Arsene 2008; Oushabi et al. 2018) and hot-water treatment (Izani et al. 2013; Ali et al. 2013) with reported improvements in physical and mechanical properties of the fibres.

Alkalisation

Alkalisation is the process of treating plant fibres with alkalis in a bid to improve their morphology and physico-mechanical properties. Alkalisation removes weak boundary layers of matter that protect the fibre's surface and that possess poor shear resistance at fibre-matrix interface (Malenab et al. 2017). Alkali treatment also leaches hemicellulose, lignin, pectin and waxy compounds leaving behind cellulose - the main structural component (Kabir et al. 2012). Consequently, the surface roughness of the fibres increases due to the appearance of micropores (Izani et al. 2013; Faizi et al. 2018). The leaching of non-structural components from the fibres enable cellulose microfibrils to better align themselves through the decrease in microfibrillar angle in the longitudinal direction - a phenomenon referred to as *microfibrillar reorientation*. This reduces stress concentration and causes improvements in the tensile resistance of the fibres (Bourmaud et al. 2013; Izani et al. 2013). Improvement in tensile strength after alkalisation is also attributed to an alkali-induced increase in crystallinity of fibre cellulose (Santos et al. 2018). The most popular alkali used for treating vegetable fibres is sodium hydroxide (Symington et al. 2008) and this is due to its ability to cause a complete lattice transformation of cellulose structure, unlike other alkalis.

While some studies (Izani et al. 2013; Faizi et al. 2018) report improvement in mechanical properties of vegetable fibres after NaOH treatment, other studies (Ozerkan et al. 2013; Meheddene et al. 2014) report otherwise and attribute it to the degradation of cellulose chains. For example, Faizi et al. (2018)

recommended dipping EFBF in 3% NaOH solution for 7 hours with an improvement in tensile strength and Young's modulus of over 100% and 14%, respectively. Izani et al. (2013) reported improvements in tensile strength and Young's modulus of 23% and 9%, respectively, for EFBF after soaking in 2% NaOH solution at room temperature for 30 minutes. Although Mydin et al. (2018), did not perform any test on (6% NaOH pretreated) coconut fibres directly, about 30% improvement in compressive strength of concrete incorporating the fibres was reported. This implies improved bonding between the concrete matrix and the coconut fibres.

No improvement in tensile strength was recorded by Sreekala et al. (1997) for NaOH-treated EFBF. However, modulus of elasticity was improved after soaking of the fibres in 5% NaOH solution for 48 hours and rinsing with plenty of water containing a few drops of acetic acid. This rinsing procedure neutralizes residual alkali on fibre surface (Osoka and Onukwuli 2015). Ozerkan et al. (2013) recommended dipping palm fibres in 2% NaOH for 1 hour at room temperature after which they were rinsed in plenty of water, then placed in an oven to dry at 60^0C for 3 hours prior to inclusion in a cementitious matrix. Although no improvement in fibre mechanical properties was noticed, the fibres were reported to be cleansed of impurities.

In summary, it suffices to say that leaching of lignin, wax, hemicellulose and other impurities from the fibres results in *microfibrillar reorientation* which reduces the microfibrillar angle. Reduced microfibrillar angle implies alignment of micro-fibrils in the longitudinal direction and hence results in improved tensile strength for the fibres. Furthermore, for a given vegetable fibre, an alkali concentration beyond a given critical concentration would cause a reaction that would embrittle the cellulose structure (Beckermann et al. 2004). In the correct concentration, however, alkali treatment decreases surface tension, increases aspect ratio and enhances bonding with matrices through either inter-diffusion, electrostatic adhesion, chemical reaction, mechanical interlock or a combination of these mechanisms (Zhou et al. 2016). This is as a result of an increase in the number of reaction sites between fibre and matrix (Ozerkan et al. 2013; Mydin et al. 2018). Although there is disparity on the moisture absorption behaviour of vegetable fibres after

alkalisation, there is agreement that alkalisation leads to enhancement in fibre purity, rougher fibre surface and improvement in fibre-matrix bond.

Silane Treatment

Silane (SiH_4) treatment, sometimes referred to as *silanization*, is a covalent coating method for modifying the surface of materials which are rich in hydroxyl groups (Boccafoschi et al. 2018). Vegetable fibres contain a high amount of hydroxyl groups which is the major factor responsible for their hydrophilic behaviour (Ozerkan et al. 2013). Their characteristic high-water absorption is one of the main factors responsible for dimensional instability and durability issues (Kabir et al. 2012). For vegetable fibres, the extent to which silane is absorbed by chemical bonding depends on the amount of free OH-radicals available in the fibre (Sreekala et al. 1997), temperature, hydrolysis time and the functional group of the silane (Zhou et al. 2016). Silane treatment has been described as an effective method for modifying fibre surfaces and for reducing water absorption in vegetable fibres (Asim et al. 2016). It is also reported as effective in improving durability and adhesion of vegetable fibres with both cementitious (Bilba and Arsene 2008) and polymeric matrices (Oushabi et al. 2018). Sreekala et al. (1997) showed that triethoxyvinylsilane reacts with water to form silanol and alcohol as shown in Eq. (1):

$$CH_2CH\ Si\ (OC_2H_5)_3 + 3H_2O \rightarrow CH_2CH\ Si\ (OH)_3 + 3C_2H_5OH \quad \ldots\ldots (1)$$

When vegetable fibres are introduced into the solution silane molecules adhere on to the OH^- groups of the fibre substrate (Bilba and Arsene 2008). The mechanism of initiating hydrophobicity in the fibres is through the development of a protective monolayer on the proton-bearing fibre surfaces thereby making fewer sites available for subsequent moisture absorption (Sreekala et al. 1997). For example, water absorption of silane treated sugarcane bagasse fibres reduced by more than 60%, thus improving cement adhesion onto the fibres (Bilba and Arsene 2008).

Goud and Rao (2013) immersed fibres of *Roystonea regia* in an acetone solution consisting 1% (v/v) 3-amino propyl-triethoxysilane for 1 hour at room temperature after which the fibres were washed with plenty of water and dried at 60^0C for 24 hours. The fibres were then used to reinforce epoxy-based

composites. Improvements of 23%, 158% and 304% in tensile strength, Young's modulus and impact strength, respectively, were recorded for the vegetable fibre-reinforced epoxy composites at a fibre inclusion of 20%. Although mechanical properties of the fibres were not studied independently, the improvement in mechanical properties of the composites implies that tensile strength of the fibres and its bonding with the matrix was enhanced by the silane pretreatment. In a similar study (Atiqah et al. 2017), about 30% improvement in tensile strength and Young's modulus of sugar palm fibres was recorded after immersing the fibres in 2% triethoxyvinylsilane dissolved in methanol-water (90:10 w/w) for 3 hours under stirring. The sugar palm fibres were washed with plenty of distilled water and left to dry in an oven for 72 hours at 60^0C prior to testing. Sreekala et al. (1997) recommended soaking EFBF in 1% triethoxyvinylsilane solution in water-ethanol ratio of 40:60 for 3 hours, then rinsing with water until a pH of between 3.5 – 4 is achieved. Due to the leaching of impurities, about 6 – 7% weight loss was observed after silane treatment of the EFBF. However, an improvement of over 45% in the tensile strength of the fibres was also reported. Generally, fibre modifications intended for polymeric matrices are also beneficial for cementitious matrices. When considering this method of treating natural fibres, using the right concentration of silane is important because excess hydrolysis and condensation reaction are possible. For high silane concentration, the presence of residual silanol groups and deficiency in hydroxyl group from the fibres will cause a gel-like precipitate over the fibres' surface, resulting in reduction in the compatibility between fibre and matrix.

Hot-water Treatment

Boiling causes leaching of soluble impurities from natural fibres thereby enhancing their cleanliness. Santos et al. (2018), after treating piassava fibres by heating 1g of the fibres in 47ml distilled water for 2, 12 and 24 hours at 75^0C recorded an improvement in crystallinity index of 32% due to the removal of lignin from the fibres. Defibrillation of the piassava fibres was also noticed after hot-water treatment. In another study by Sellami et al. (2013), hot-water treatment of diss fibres was reported to improve bonding between the fibres and cementitious matrix due to the elimination of water-soluble sugars from an initial concentration of 30.78% to 0.72%. The diss fibres were boiled in tap water at 100^0C for 4 hours. A diss/cement proportion of 4:1 was used in concrete at a water/cement ratio of 0.7. Improvements in

mechanical properties over untreated diss-concrete were recorded as 200% and 170% for compressive strength and flexural strength respectively. No improvement was found for water absorption of treated diss fibres. Ali et al. (2013) improved the bond strength between coconut fibre and concrete by boiling the fibres in water for 2 hours. Fibre tensile strength, fibre-concrete bond strength and fibre toughness were improved by 34%, 184% and 55%, respectively.

Hot water treatment is cheaper than alkalisation and silanization especially based on the fact that it is void of the management of chemical waste-water effluents. Hot-water treatment was also reported to be superior to sodium alginate ($NaC_6H_7O_6$) and calcium chloride ($CaCl_2$) treatments of coconut fibres.

Although studies on other types of fibres (derived from *Elaeis guineensis*) with possible applications abound, research focus on OPBF is quite recent despite its impressive physical and mechanical properties. Recent studies have shown that the fibres can be used to reinforce cementitious composites in a bid to achieve eco-friendly construction (Momoh and Dahunsi 2017; Momoh and Osofero 2019). However, the mechanical properties of OPBF-reinforced concrete tend to reduce with time due to factors such as poor bonding between OPBF and concrete, moisture-induced dimensional instability and alkali-induced degradation of the fibres. There is, therefore, the need to investigate treatments that could enhance the durability of OPBF which is the aim of the present study. This study investigates the effects of alkali treatment (alkalisation), silane treatment (silanization) and hot-water treatment on some physical and mechanical properties of OPBF. The fibres were soaked in different concentrations of alkali (sodium hydroxide), silane (triethoxyvinylsilane) and hot water each for different durations. The effects of these treatments were measured in terms of fibre tensile strength, modulus of elasticity, water absorption, cross-sectional dimension, surface morphology and crystallinity index. Recommendation concerning the feasibility of using the treatment methods in cement and polymeric composites is made. Treatment has been focused on OPBF stored at room temperature for about 400 days after harvesting from the oil palm tree.

Materials and Methods

OPBF (sourced from *Elaeis guineensis*) were obtained from *Rice and Spice*, Aberdeen, UK in the form of broom units. Selection of blemish-free fibres was done by visual inspection and hand-picking. For each OPBF, lengths of 200mm (from the fibre head) were cut and grouped into bunches of 70 fibres each for the 3 different treatments (i.e., 210 fibres in total). Three (3) identical replicants were tested for tensile strength per treatment, concentration and duration (i.e., 132 in total) while the remaining 78 fibres were used for x-ray diffraction (XRD), scanning electron microscopy (SEM) and water absorption analysis. Average values and corresponding standard deviations for each measured property were calculated. Fig. 1 illustrates four OPBF classification in terms of length from fibre-head as defined in a previous study (Momoh and Osofero 2019). The OPBF were subjected to three treatment types, namely, alkalisation, silane treatment and hot-water treatment. The alkali, sodium hydroxide (NaOH) and the silane (deposition grade triethoxyvinylsilane) used were obtained from *Sigma-Aldrich* UK Ltd. After treatment, three fibres each from both untreated and treated batches were prepared for tensile test, water absorption test, XRD test and SEM. In other words, the effect of the treatments on OPBF were measured in terms of tensile strength, water absorption behaviour, dimensional changes in fibre cross-section, fibre surface morphology and changes in crystal structure. *Araldite* epoxy glue, obtained from *Gibb Tools*, Aberdeen, UK, was used to provide hardened fibre ends for the tensile test. Details of treatments and preparation of OPBF samples for the different tests are given in the following sections.

OPBF treatments

Alkalisation

The fibres were immersed in 2%, 4%, 6% and 10% sodium hydroxide solution. Immersion times for each alkali solution were 30, 120, 240, 480, 1440 and 2880 minutes. At the respective durations, they were washed with plenty of water from a running tap and dried in an oven at 60 ± 3^0C for 8 hours.

Silane treatment

The fibres were immersed in a water/ethanol mix (of 40/60 respectively) containing 1% and 3% triethoxyvinylsilane. Immersion times for each silane concentration were 60, 120, 240, 480, 1440 and 2880

minutes. The fibres were then removed and washed with plenty of water from a running tap and dried in an oven at 60 ± 3^0C for 8 hours.

Hot-water treatment

The fibres were immersed in boiling water (at 100^0C) for time durations of 15, 30, 60 and 120 minutes. At the end of the respective durations, they were removed, rinsed with plenty of tap water and dried in an oven at 60 ± 3^0C for 8 hours.

Tensile strength test

Three OPBF were picked from each batch of untreated and treated fibres and prepared for tensile strength test. Healthy-looking fibres were selected by visual inspection and trimmed to 150mm. Due to the low radial rigidity of OPBF, the grips of the testing machine squashed sample ends, thereby causing stress concentration and premature failure at the section just around the grips. Hence a method of avoiding this was devised by dipping each end of the fibres into *Alradite* epoxy glue such that a bulb of glue hardened sufficiently at both fibres ends. A bulb dimension of about 20 mm and 7 mm in length and thickness respectively was achieved (see Fig. 2). A gauge-length of 110 mm was adopted throughout the tensile strength test for all OPBF samples. Tensile testing of the fibres was carried out using a Hounsfield universal testing machine (Model H10KS). Each OPBF was inserted into the grips at the bulb ends and secured in a vertical position. Testing was carried out in accordance with ASTM D4761-13 (2013) in displacement control at 2.5mm/min. The stress-strain relationship used for all OPBF samples was calculated based on the smallest cross-sectional area of each fibre as fibre failure either occurred or was initiated at such points. Cross-sectional areas of the samples were measured using a digital vernier calliper with an accuracy of 0.01 mm.

Water absorption test

The water absorption behaviour of untreated and treated OPBF were investigated in accordance with ASTM D570–98 (2018). All OPBF samples were dried in an oven at 53^0C and allowed to cool at room temperature before weighing them to the nearest 0.01g. Each sample was immersed in tap water at room

temperature. At designated times they were removed from the water, wiped with soft tissue paper and weighed on a digital weighing balance. The measurement process was ensured within 1 minute of removal from water. The specimens were weighed at 15, 30, 60, 120, 240, 480, 1880 and 2440 minutes of immersion. Moisture absorption was calculated as the difference in weight (in percentage) before and after immersion. The percentage water absorption *w(t)* of untreated and treated OPBF was calculated using Eq. (2):

$$w(t) = \frac{m_t - m_0}{m_0} X\ 100\%, \ldots \ldots \ldots \ldots \ldots \ldots \ldots (2)$$

where m_0 and m_t are the mass of OPBF sample before and after immersion respectively.

Scanning Electron Microscopy (SEM)

SEM images of treated and untreated OPBF were obtained using a *CarlZeiss GeminiSEM 300VP* scanning electron microscope. A 20 nm-thick carbon coating was first applied over the samples followed by approximately 10nm-thick sputter coating of gold/palladium alloy (60% Au and 40% Pd). This was done to enhance the conductivity of the samples. Images of cross-sections, longitudinal sections and surface of OPBF were acquired and examined. Electron Microscopy was performed using the facilities at the Aberdeen Centre for Electron Microscopy, Analysis and Characterisation (ACEMAC), University of Aberdeen UK.

X-ray diffraction (XRD) analysis

Crystallinity of OPBF was determined by powder XRD method using a *Panalytical X'Pert* diffractometer with a generator setting of 45 kV and current flow of 40 mA. Untreated and treated OPBF samples were pulverised to particle size passing through 50 µm sieve with the aid of a laboratory mortar and pestle. Scanning of samples was carried out with CuKα radiation of wavelength 0.1542 nm at 2θ angle range of 10^0 - 80^0 and at a step size of 0.013^0. Total scan time for each sample was 30 minutes. The crystallinity index (*CI*) was calculated by Segal empirical method (Segal et al. 1959; Dasong and Mizi 2010; Pandiarajan et al. 2018) as shown in Eq. (3):

$$CI = \frac{I_{002} - I_{am}}{I_{002}} \text{ x } 100\%, \ldots \ldots \ldots \ldots \ldots \ldots \ldots \ldots \ldots \ldots \ldots \ldots \ldots \ldots \ldots \ldots (3)$$

where I_{002} is the maximum diffraction intensity of both crystalline and amorphous materials and I_{am} is the minimum diffraction intensity of amorphous material. XRD analysis was performed using the facilities at ACEMAC, University of Aberdeen UK.

Results and Discussion

OPBF Structure

SEM images of OPBF before and after treatments are shown in Figs 3-5 with the fibres comprising a densely packed outer layer and a core consisting of tubule-like phloems and xylems in the range of 25-25000 μm^2 in cross-section. Average wall thickness of the tubules is 1μm with each tubule firmly bounded with adjacent tubules by lignin. The tubules located at the centre of the OPBF cross-section are such that they have a series of side-way openings into adjacent surrounding tubules as shown in the longitudinal sections through untreated OPBF (see Fig. 3 (a2)). This natural functionally graded mesh-like arrangement makes OPBF peculiar in its bending behaviour by snapping back to position (in vibration) when one end is held fixed and the other released instantaneously from a displaced position. Fig. 3 presents the longitudinal sections through untreated and alkali treated OPBF, Fig. 4 presents the surface topography of the skin of OPBF and Fig. 5 shows the cross-sections.

Surface topography

During alkalisation and hot-water treatment of OPBF, there occurred a change in colour of the sodium hydroxide solution from colourless to reddish-brown (see Fig. 6). This was due to both hot-water and alkali induced leaching of impurities, wax and lignin from the fibres. Consequently, the weak boundary layer of the fibre surface wore off, thereby exposing micropores. This occurs through the attack of carbon atoms of ester bonds by the hydroxide ions from the alkali. The ester bonds are located either between two lignin components or between a lignin and a carbohydrate component. The resulting tetrahedral intermediates are unstable ~~in nature~~ and hence collapse when oxygen atoms expel alkoxides from carboxylic acid. The expelled alkoxides then removes the protons of the carboxylic acid thereby causing irreversible hydrolysis

of the ester bonds and the eventual degradation of lignin. This process of fibre surface wear-off by alkali is consistent with the study of Modenbach and Nokes (2014). Eq. (4) presents a highly simplified reaction mechanism between vegetable fibres and NaOH (Zhou et al. 2016).

$$\text{Fibre} - OH + NaOH \rightarrow \text{Fibre} - O^{-}Na^{+} + H_2O + \text{impurity} \quad \ldots (4)$$

The effect of alkali on OPBF morphology is further observed in the SEM images of Figs 4 and 5. In Fig. 4 (c1 and c2) a rougher but cleaner surface topography is shown to have occurred after 48 hours of 6% NaOH. Beyond a NaOH concentration of 6%, removal of lignin and impurities is followed by degradation of cellulose structure, thereby causing cracking of the OPBF as shown in the cross-section images presented in Fig. 5 (h1 and h2) and the longitudinal section images in Fig. 3 (b1 and b2). Furthermore, the leaching of lignin, wax and impurities from the fibres was succeeded by fibre shrinkage and can also be observed in the cross-section shown on Fig. 5 (h1 and h2). The leaching of lignin and impurities from vegetable fibres during alkali treatment reduces the angle of orientation between the microfibrils constituting the fibre. This re-alignment increased the packing of the microfibrils and therefore a reduced (but denser) cross-section for the OPBF as revealed in Fig 5 (h1 and h2). The appearance of micropores on the surface of alkali treated OPBF is also consistent with other studies (Izani et al. 2013; Osoka and Onukwuli 2015; Hestiawan et al. 2016)

The reaction between triethoxyvinylsilane and water results in the formation of silanol and alcohol as shown in Eq. (1). Silanol ($CH_2CHSi(OH)_3$) adhered onto the hydroxyl group (OH^-) of the OPBF substrate thereby providing a covalent coating over the OPBF surface. A comparison between Fig. 4 (c1 and c2) and Fig. 4 (e1 and e2) shows a levelling up of the undulations on the untreated fibre-surface by silane coating. This may be advantageous for composites relying on chemical adhesion as the governing bond parameter between fibres and matrix. In cement composites where mechanical interlock between reinforcement and matrix is desired, it is important to determine the correct concentration of silane for a particular vegetable fibre. Nevertheless, silane treatments prevent the competition for water between the hydration reaction of cement matrix and water absorption of vegetable fibres, thereby enhancing the dimensional stability and bond strength between the fibres and matrix. Furthermore, water-proofing of OPBF would prevent

dissolution of fibre impurities and consequently reduce setting time for a cementitious matrix. Swelling of OPBF was observed and measured in terms of increase in cross-sectional area, to be between 1.4 - 28% (Fig. 7), which is similar to the findings of Ramamoorthy et al. (2015) for silane treatment of regenerated cellulose fibres.

Hot-water treatment caused the escape of lignin molecules from within the fibres and the deposition of the same on the surface of the fibres. Fig. 4 (f1 and f2) shows the agglomeration of lignin on the OPBF surface. In the case of alkalisation, lignin dissolved off the surface of the fibres. Since lignin is incompatible with both polymer and cement matrices, it is recommended to either thoroughly wash the fibres after hot water treatment or extend the treatment duration. The effect of pressure build-up within the OPBF due to the treatment temperature (100^0C) resulted in radial cracking (see Fig. 5 (n1 and n2)). To avoid damage to the fibres, hot-water treatment may be carried out at a temperature lower than 100^0C.

Alkalisation and hot-water treatment were more effective treatments for enhancing fibre purity. On the other hand, the reduction in water-absorption for silane treated OPBF indicates that silane treatment was a more effective water-proofing option. However, hot-water treatment is cheaper and more environmentally friendly when the cost of the treatment chemicals and management of effluents are considered.

Water absorption behaviour

Fig. 8 presents a graph of percentage water absorption *w(t) versus* square root of time $\sqrt{t}$ for untreated and selected treated fibres. Both the untreated and treated OPBF absorbed water rapidly, but at a consistent rate, for the first 25 minutes, thereby resulting in an initial linear relationship between time and percentage of water absorption. This gradually changed to an equilibrium plateau as the time rate of water absorption reduced, thereby signifying Fickian diffusion behaviour (Célino et al. 2013). The leaching of lignin, oil, waxes and impurities from OPBF created more intermolecular spaces for increased water absorption.

It was also observed that alkali treated OPBF underwent swelling between 0 and 20 minutes of immersion in water. OPBF are large fibres and contain cavities, hence it is difficult to eliminate residual NaOH in the fibres after treatment. Soaking OPBF in water for 24 hours or more after NaOH-treatment could eliminate

residual alkali. Sodium ions from the alkali widened the pores on the fibres and penetrated lattice planes to separate them. This resulted in a new Na-cellulose-I lattice structure with a larger distance between cellulose molecules (Zannen et al. 2014). Residual Na^+ ions causes high swelling of OPBF and increased water absorption for alkali treated fibres. Consequently, the OH-groups of the cellulose transform into ONa-groups (see Eq. 4). While the elimination of amorphous constituent of the fibres exposed more OH^- reaction sites on cellulose to attract water, silane treated OPBF were overlaid by a thin film of polysiloxane molecules which sealed off the pores of the surfaces, hence reducing hydrophilicity (Bilba and Arsene 2008). Water absorption of untreated OPBF was 48% after 48 hours of immersion. Average percentage increase in water absorption was 40% for alkali treated OPBF and a maximum increase of 80% was recorded when samples were treated with 4% NaOH for 48 hours. For hot water treatment, maximum increase in water absorption of 9% was recorded for samples treated at 100^0C for 2 hours. For hot-water treated OPBF, dissolved lignin and fibre impurities from within the fibres were observed to clog the pores at the surface (Fig 4-f2), hence preventing water penetration akin to alkali treated fibres. Average reduction in percentage water absorption for silane treated OPBF at 48 hours was recorded as 4%.

The trend of diffusion of water molecules at room temperature into the OPBF was evaluated by taking into consideration the main factors controlling fibre-water interaction, which are diffusion, permeability and sorption (Sreekala et al. 2001). For one-dimensional moisture absorption, total moisture content G is expressed in Eq. (5) (Dharkal et al. 2006; Muñoz and García-Manrique 2015):

$$G = \frac{w_t - w_i}{w_s - w_i} = 1 - \frac{8}{\pi^2} \sum_{q=0}^{\infty} \frac{1}{(2q+1)} \exp\left(-\frac{(2q+1)^2 \pi^2 D t}{h^2}\right), \ldots \ldots \ldots \ldots \ldots \ldots . \ldots \ldots \ldots \ldots \ldots \ldots \ldots (5)$$

where w_t is the weight of sample at an instantaneous time (t), w_i is the initial weight of moisture in the sample, w_s is the weight of moisture in the sample at full saturation (saturation moisture content), D is the diffusion coefficient, h is the thickness of sample, t is the time and q is the summation index.

Eq. (5) can be solved in terms of percentage moisture content thus:

$$\frac{w_t}{w_s} = 4\sqrt{\frac{tD}{\pi h}}, \ldots \ldots \ldots \ldots \ldots \ldots \ldots \ldots \ldots \ldots \ldots \ldots \ldots \ldots \ldots \ldots \ldots \ldots \ldots \ldots \ldots \ldots \ldots \ldots \ldots \ldots \ldots \ldots \ldots \ldots . . \ldots (6)$$

where w_s and w_t are the saturation moisture content and moisture content ~~of~~ at any instantaneous time (t) of the specimen. The diffusion coefficient (*D*) was calculated for both treated and untreated OPBF by expressing Eq. (6) in terms of *D* such that;

$$D = \pi \left(\frac{hk}{4w_s}\right)^2, \ldots \quad (7)$$

where *k* is the initial slope of a plot of the percentage water absorption *w(t) vs* square root of time *(t)*, w_s is the saturation moisture content and *h* are the thickness (in this case, the diameter of cross-section) of the OPBF sample. Table 1 shows the calculated diffusion coefficients for untreated and selected treated OPBF.

Diffusion coefficient *D* of untreated OPBF was found to be 0.43 times the value reported for *Raffia vinifera* fibres (Tagne et al. 2014), 14.4 times that of sisal fibres, 7.7 times that of hemp fibres, 27.5 times that of jute fibres and 25.9 times that of flax fibres (Célino et al. 2013). However, OPBF possesses inherently low saturation moisture content.

Tensile behaviour

Fig. 9 shows the effect of alkalisation on tensile strength of OPBF. Effect of alkalisation on tensile strength was noticed after 4 hours of 2% NaOH treatment. Maximum improvement in tensile strength (60%) was recorded at 6% NaOH at 48 hours. The NaOH concentration of 2% showed more consistent improvement in tensile strength with an optimum time of 8 hours. At 10% NaOH, tensile strength reduced with an increase in treatment time. Tensile strength results (Fig. 9) also showed some values for treated fibres as lower than that of the untreated fibres. The inherent heterogeneity of the fibres themselves ~~have~~ resulted in variation in tensile strength. Studies have shown that fibres from the same plant species vary widely in their physical and mechanical properties even in their untreated forms. Factors responsible for these variations are the climatic condition of the region of cultivation of parent plant (Anyakora et al. 2017), age of the parent plant, age of fibres after extraction from the parent plant and the predominant cellulose type in the fibres (Wang et al. 2007). Secondly, plants possess cell-based mechanosensors that transform environmental stimuli (e.g. wind) into biologically recognised signals thereby controlling the allocation of plant tissue to certain parts (Nogata and Takahashi 1995). This implies that plant fibres at different

386 locations of the same plant may further display varying stiffnesses and tensile strengths. Furthermore,
387 selection of healthy fibres was carried out by visual observation which may have allowed fibres with
388 internal defects to be undetected. These might explain some of the unusually low values of tensile strength
389 recorded for the treated fibres. Notwithstanding, an increase in tensile strength with treatment duration is
390 generally observed.

391 From Fig. 10 maximum strain at maximum tensile strength (40%) was recorded at 2% NaOH at 4 hours.
392 Beyond 8 hours of treatment, the effect of alkalisation on strain of OPBF is negligible. The loss of
393 impurities, wax and lignin from OPBF caused the reduction in the cross-section of the fibres. At 48 hours
394 of alkalisation, reduction in cross-sectional areas were 33%, 67%, 55% and 35% for 2%, 4%, 6% and 10%
395 NaOH respectively, (see Fig. 11), along with excessive cracking (see Fig. 5 (h1)). This range of reduction
396 in cross-sectional area agrees with previous studies (Sreekala et al. 1997; Meheddene et al. 2014). Aside
397 from impurities, microfibrils of vegetable fibres consists of two regions: the crystalline region with highly
398 ordered cellulose molecules, (which makes up 2/3 of the total cellulose) which is resistant to hydrolysis by
399 acids and enzymes, and the amorphous region which is easily hydrolysable (Rambo et al. 2015). It can be
400 inferred therefore that beyond 6% NaOH concentration, amorphous cellulose chains underwent partial
401 hydrolysis and were removed from OPBF. This led to a further reduction in cross-sectional areas of the
402 fibres at 10% NaOH. The increase in tensile strength is, therefore, partly due to the increase in crystallinity
403 of the cellulose structure of the OPBF. Higher concentrations of alkali would, however, attack the cellulose
404 crystals resulting in loss of overall fibre strength and stiffness (Izani et al. 2013; Beckermann et al. 2004).

405 Furthermore, the improvement in the tensile strength of the treated OPBF was also due to micro-fibrillar
406 reorientation. Loss of lignin resulted in a reduction in micro-fibrillar angle thereby causing re-alignment of
407 the microfibrils within the fibres. The realignment of microfibrils can be noticed as an increase in strain
408 (between 2 – 4 hours of alkali treatment in Fig. 10) and occurred along the axis of fibre-loading, thereby
409 reducing stress concentrations. Consequently, there was an enhancement of fibre tensile strength. Micro-
410 fibrillar reorientation was more pronounced at the beginning of the tensile tests, after which OPBF behaves
411 like a perfectly elastic material until sudden brittle failure (see Fig. 12). A marked difference is however

412 noticeable between the failure modes of alkali treated OPBF and silane treated OPBF. While the alkali
413 treated fibres failed in pure tension, silane treated fibres failed in a “tensile-shear-delamination” manner
414 (see Fig. 13). The chemical reaction between silane and hydroxyl groups from the fibre surface is covalent
415 and cross-linked. With the availability of reaction time, a three-dimensional polymerized network is formed
416 thereby creating strong intermolecular adhesion at the silane-fibre interface (Ratner and Hoffman 2013).
417 Unlike alkali treated samples which fail at the smallest cross-section when subjected to axial tension,
418 silane-coating caused some redistribution of tensile stresses throughout the fibres such that defibrillation is
419 forced to occur. This phenomenon resulted in higher tensile strengths and strains for silane treated OPBF
420 (see Fig. 14). Effect of 1% silane on tensile strength of OPBF was negligible, but at 3% silane
421 improvements in tensile strength were up to 33%, 50%, 40%, 59% and 34% at 2, 4, 8, 24 and 48 hours,
422 respectively. Since silane treatment does not show marked improvements in the tensile strength of OPBF
423 beyond 24 hours, optimum treatment time of 24 hours is recommended. Fig. 15 shows strain at failure for
424 silane treated OPBF and Fig. 7 shows the measured cross-sectional areas after silane treatment for each
425 treatment duration and silane concentration. Apart from swelling noticed at 8 hours of 1% silane treatment,
426 the effect of silane on the cross-sectional dimension of OPBF is negligible.

427 Fig. 16 shows the tensile strengths of hot-water treated OPBF. Maximum increase in tensile strength of
428 66% was recorded at 30 minutes. Strain at maximum tensile strength was increased by 17% (see Fig. 17).
429 Reduction in cross-sectional area was noticed from 1 hour of hot-water treatment as shown in Fig. 18. A
430 gradual change in colour of the water was observed from been clear to reddish-brown signifying the
431 leaching of impurities from the fibres. This is similar to the dissolution of impurities from OPBF during
432 alkalisation (see Fig. 6). No improvement in the tensile strength of the fibres was recorded beyond 30
433 minutes; hence it is recommended that optimum treatment time for OPBF at 100^0C is 30 minutes.

434 Similar to the alkali treatment, tensile strength results for both silane and hot-water treatments show some
435 reduction for treated fibres at low treatment concentration and duration. This is due (as explained earlier for
436 alkali treated OPBF) to the presence of defects or the inherent heterogeneity of the fibres themselves and
437 not the treatment. Due to the variability of properties between vegetable fibres, it is important while

planning for these types of studies to maintain a careful selection even among fibres that are blemish-free. The inherent variability in OPBF discovered in this study also implies that testing a higher number of identical samples per treatment concentration and duration would improve the reliability of the results. Due to these findings, a higher number of samples will be considered in future studies.

Relationship between tensile strength and elastic modulus

OPBF have been reported to be superior to steel in terms of tensile strength-to-weight ratio (Momoh and Osofero 2019). Although research on OPBF is scarce and only recent, factors responsible for its relatively high tensile strength may include high cellulose content, low microfibrillar angle and dense packing of the microfibrils. Fig. 19 presents the relationship between Young's modulus and tensile strength for untreated and treated OPBF. Alkali treated OPBF shows a higher slope which indicates that reduction in strain is more pronounced compared to silane and hot-water treated fibres. In other words, as the concentration of NaOH increases beyond 6%, excessive embrittlement of the fibres occurs and strain at failure is reduced thereby resulting in higher values of elastic modulus. Untreated fibres underwent higher strains. Eqs (8) - (11) were derived from the lines of best-fits (Fig. 19) for each treatment method.

$E_{opbf} = 0.0146\,\sigma + 3.43 \quad (R^2 = 0.9899)$ ……(8)

$E_{hot\text{-}water} = 0.0258\,\sigma \quad (R^2 = 0.9080)$ ……(9)

$E_{silane} = 0.0225\,\sigma \quad (R^2 = 0.5914)$ ……(10)

$E_{alkali} = 0.0264\,\sigma \quad (R^2 = 0.7329)$ ……(11)

where E_{opbf}, $E_{hot\text{-}water}$, E_{silane}, E_{alkali} are the elastic modulus (in GPa) of untreated, hot-water treated, silane treated and alkali treated OPBF respectively and σ is the respective tensile strength (in MPa). The R-squared values of untreated and hot-water treated OPBF indicates a good fit between the models and the experimental data. Although the fits between data and models for alkali and silane treated OPBF are not as good as that of untreated and hot-water treated OPBF, the derived equations can be useful in predicting elastic modulus of OPBF values from known tensile strengths.

X-ray diffraction analysis

XRD analysis revealed the change in the crystallinity of OPBF for the different treatment methods. Fig. 20 and Table 2 presents the graph and results of the diffraction analysis respectively. Crystallinity index of untreated OPBF was obtained as 20.2%. Crystallinity index of OPBF was improved by 44%, 25% and 4% for alkalisation (6% NaOH for 48 hours), silane treatment (3% silane for 48hours) and hot-water treatment (at 100^0C for 2 hours), respectively. Increase in crystallinity was due to degradation of hemicellulose, lignin, wax and other impurities (Santos et al. 2018; Terán-Hilares et al. 2016). Since OPBF is a giant fibre with size over 90 times that of other natural fibres, it would take a longer treatment time to achieve higher improvements in crystallinity. The range of 2θ angle at which the peak heights of the crystalline region (I_{002}) and the amorphous region (I_{am}) occurred is 21.35^0 - 21.96^0 and 16.68^0 – 18.41^0 respectively. This signifies that *cellulose I* is the predominant cellulose type in OPBF (Deraman et al. 2001; Souza et al. 2016). Also, an observation of the XRD curves shows only slight changes in the 2θ angles at which the peak intensities of diffraction occur for both treated and untreated fibres. This implies that no change in cellulose form (crystal structure) occurred. A total transformation of plant cellulose crystal structure is rare (Fortea-Verdejo et al. 2017), however, the inadequacy of time for treatments to reach inner parts of the OPBF is a contributory factor in this study. Therefore, in treating natural fibres for improved crystallinity, four (4) main factors should be acknowledged, namely, (i) thickness of fibre, (ii) concentration of treatment solution, (iii) duration of treatment and (iv) fibre sorption behaviour.

Although Dasong and Mizi (2010) advised that crystallinity index be used only in comparing the order of crystallinity for vegetable fibres, degree of crystallinity has been reported to be proportional to Young's modulus (Wei and Meyer 2014). A higher crystallinity index could be considered as a factor for choosing natural fibres for composite manufacturing. NaOH-treatment showed the highest improvement in crystallinity which corroborates the findings of other studies (Van de Weyenberg et al. 2006; Deraman et al. 2001; Masniroszaime et al. 2018). Hot-water treatment may not be effective in improving crystallinity (Santos et al. 2018) but an increased boiling duration beyond 2 hours at a temperature less than 100^0C may be beneficial for dissolving and flushing out impurity, accumulated lignin on fibre surface and trapped lignin within the fibre structure. However, an extended build-up of pressure in the OPBF cavities (due to

prolonged heating) can cause damage to its internal structure. An optimum temperature for hot-water treatment of OPBF needs to be investigated.

Crystallinity index of untreated OPBF obtained in this study (Table 2) is close to 20.27% and 27.2% obtained for sisal fibres (Wei and Meyer 2014) and pressed oil palm mesocarp fibres (POPMF) (Souza et al. 2016), respectively. Although Shah (2013) reported crystallinity index of 20-30% for oil palm fibres, varying values of crystallinity index are reported in other studies such as 41.58% (Kuthi et al. 2015), 53±3% (Deraman et al. 1999) and 75.06% (Pangsang et al. 2019) for EFBF and 44.61% OPMF (Chieng et al. 2017). Usually, natural fibres even of same species show varying inherent properties, however, a major factor for this variation in crystallinity could be the particle size and degree of purity of the pulverised fibres before testing.

Momoh and Osofero (2019) presented the first attempt at evaluating bond strength between untreated OPBF and concrete. It was shown that factors such as degradation of weak fibre-surface, moisture-induced dimensional instability and cement-embrittlement of OPBF were responsible for loss in bond strength with concrete. Although the bond behaviour of treated OPBF with concrete was not evaluated in this study, the findings reveal at least four (4) fibre improvements that will enhance bonding between treated OPBF and concrete, namely: elimination of impurities from the fibres, reduction in water absorption (for silane treated OPBF), rougher surface morphology and improvement in tensile strength of the fibres. Further study on silane treatment following either alkali or hot-water treatment is recommended. While alkali treatment or hot-water treatment enhances fibre purity, silane treatment enhances fibre hydrophobicity. The dual action of such combined treatments would result in more dimensionally stable fibres with surfaces that are void of impurities thereby enhancing bonding and improving the mechanical performance of the composite.

The major concerns regarding treatment methods employed in this study are the cost of treatment and environmental implications. While water is cheap, the cost of energy for heating must be taken into consideration. To tackle this, renewable sources of energy can be employed. The huge waste biomass from the oil palm industry is a potential source of cheap fuel. Sodium hydroxide and silane, on the other hand, are relatively expensive and treatment of large effluents of wastewater may add to the overall treatment

cost. However, recycling and recovery of these chemicals from their effluents are also possible. These could reduce the cost of treatments and increase the margin between cost and the target improvements sought. Finally, since the ratio of the fibres to the treating liquid (sometimes referred to as "solid-loading") affects the reaction rate between chemical and fibres and also the efficiency of the treatment (Modenbach and Nokes 2014), an optimum solid-loading should be studied for each treatment method. These considerations will be addressed in subsequent studies by the authors.

Finally, due to the inherent heterogeneity of vegetable fibres, variability of properties between fibres of the same plant species occurs. It is therefore important while planning to maintain a careful selection even among fibres that are blemish-free when they are used in construction.

Conclusions

Research on OPBF is scarce and recent. This study has provided an insight on possible enhancement techniques on this new palm fibre. The effect of alkali, silane and hot-water treatments on some physical and mechanical properties of OPBF (ribs of the leaflets of oil palm tree) were carried out. This was achieved by assessing water absorption, tensile strength, scanning electron microscopy (SEM) and x-ray diffraction analysis (XRD) of untreated and treated OPBF. Consequently, the following key findings are highlighted:

- Alkalisation and hot-water treatment are effective ways of cleaning OPBF from impurities such as oil and wax,
- Improvements in tensile strength and elastic modulus of up to 60% and 65%, respectively, were obtained at 48 hours with an alkali concentration of 6% NaOH at room temperature. Alkali concentration greater than 6% leads to excessive delignification of OPBF and thus damages OPBF,
- Silane treatment water-proofs OPBF surface such that water absorption is reduced. The optimum recommendation for silane treatment OPBF is 3% silane for 24 hours at room temperature which results in up to 60% improvement in tensile strength and 11% reduction in water absorption,

- Hot-water treatment is more environmentally friendly with optimum treatment time of 30 minutes at 100^0C resulting in 40% improvement in tensile strength,
- Alkalisation and hot-water treatment are more effective when purity and increased surface roughness of OPBF are essential while silane treatment is a more effective water-proofing option,
- Water absorption behaviour of OPBF obeys Fickian theory of diffusion.

Further study on silane treatment following either alkali or hot-water treatment is recommended. A combined purifying and water-proofing effect would be beneficial for further enhancement of physico-mechanical properties of the fibres which, are also advantageous for polymeric composites. Furthermore, a higher number of identical OPBF samples per treatment concentration and duration would improve the reliability of the obtained results. Treatment of OPBF would enhance production of environmentally friendly sustainable natural fibre-reinforcements for cementitious composites like lintel beams, roof tiles, building claddings and facades. The natural morphology of OPBF makes it stand out as possible reinforcement for insulation panels.

Data availability statement

Some or all data, models, or code that support the findings of this study are available from the corresponding author upon reasonable request. These include xlsx files from which manuscript figures were derived.

Acknowledgements

The authors would like to thank the Petroleum Technology Development Fund (PTDF) of Nigeria for sponsoring this research.

Conflict of Interest

The authors have no conflict of interest to declare.

Notation

The following symbols are used in this paper:

- CI = crystallinity index;
- D = diffusion coefficient;
- E_{opbf} = Young's modulus of untreated fibres;
- E_{alkali} = Young's modulus of alkali treated fibres;
- $E_{hot\text{-}water}$ = Young's modulus of hot-water treated fibres;
- E_{silane} = Young's modulus of silane treated fibres;
- G = total moisture content;
- I_{002} = maximum diffraction intensity of entire material;
- I_{am} = minimum diffraction intensity of amorphous material;
- R^2 = coefficient of determination;
- h = thickness of sample;
- k = slope of linear portion of $w(t)$ versus $\sqrt{t}$ curve;
- m_0 = initial mass of fibres;
- m_t = mass of fibres at a given time t;
- q = summation index;
- $w(t)$ = percentage water absorption at a given time t;
- w_t = weight of sample at a given time t;
- w_i = weight of moisture in sample;
- w_s = weight of moisture in sample at full saturation;
- σ = tensile strength of fibres;
- π = 3.14159.

References

Ali, M., X. Li, and N. Chouw. 2013. "Experimental investigations on bond strength between coconut fibre and concrete." *Materials and Design* 44: 596-605. doi:10.1016/j.matdes.2012.08.038.

Anyakora, A. N., O. K. Abubakre, E. Mudiare, and M. A. T. Suleiman. 2017. "Effect of fibre loading and treatment on porosity and water absorption correlated with tensile behaviour of oil palm empty fruit bunch fibre reinforced composites." *Advances in Materials Research* 6 (4): 329-341. doi:10.12989/amr.2017.6.4.329.

Ardanuy, M., J. Claramunt, and R. D. T. Filho. 2015. "Cellulosic fiber reinforced cement-based composites: A review of recent research." *Construction and Building Materials* 79: 115-128. doi:10.1016/j.conbuildmat.2015.01.035.

Arsène, M., K. Bilba, and C. Onésippe. 2017. "Treatments for viable utilization of vegetable fibers in inorganic-based composites." In *Sustainable and Nonconventional Construction Materials using Inorganic Bonded Fiber Composites*, 69-123. Amsterdam, Netherlands: Woodhead Publishing. doi:doi.org/10.1016/B978-0-08-102001-2.00004-8.

Asim, M., M. Jawaid, K. Abdan, and R. M. Ishak. 2016. "Effect of alkali and silane treatments on mechanical and fibre-matrix bond strength of kenaf and pineapple leaf fibres." *Journal of Bionic Engineering* 13 (1): 426-435.

ASTM D4761-13. 2013. *Standard test methods for mechanical properties of lumber and wood-base structural material*. ASTM International, West Conshohocken, PA, USA.

ASTM D570-98. 2018. *Standard test method for water absorption of plastics.* ASTM International, West Conshohocken, PA, USA.

Atiqah, A., M. Jawaid, M. R. Ishak, and S. M. Sapuan. 2017. "Effect of alkali and silane treatments on mechanical and interfacial bonding strength of sugar palm fibers with thermoplastic polyurethane." *Journal of Natural Fibers* 15 (2): 251-261. doi:10.1080/15440478.2017.1325427.

Beckermann, G. W., K. L. Pickering, and N. J. Foreman. 2004. "The processing, production and improvement of hemp-fibre reinforced polypropylene composite materials." *Proceeding of 2nd Internation Conference on Structure, Processing and Properties of Materials.*

Bilba, K., and M.-A. Arsene. 2008. "Silane treatment of bagasse fiber for reinforcement of cementitious composites." *Composites Part A: Applied Science and Manufacturing* 39 (9): 1488-1495. doi:10.1016/j.compositesa.2008.05.013.

Boccafoschi, F., L. Fusaro, and M. Cannas. 2018. *Immobilization of peptides on cardiovascular stent.* Woodhead Publishing. doi:10.1016/B978-0-08-100496-8.00016-0.

Bourmaud, A., C. Morvan, A. Bouali, V. Placet, P. Perre, and C. Baley. 2013. "Relationships between micro-fibrillar angle, mechanical properties and biochemical composition of flax fibers." *Industrial Crops and Products* 44: 343-351.

Célino, A., S. Fréour, F. Jacquemin, and P. Casari. 2013. "Characterization and modeling of the moisture diffusion behaviour of natural fibres." *Journal of Applied Polymer Science* 130 (1): 297-306. doi:0.1002/app.39148.

Chieng, B. W., H. S. Lee, N. A. Ibrahim, Y. Y. Then, and Y. Y. Loo. 2017. "Isolation and characterization of cellulose nanocrystals from oil palm mesocarp fiber." *Polymers* 9 (335): 1-11.

Claramunt, J., F. J. Lucía, H. Ventura, and M. Ardanuy. 2016. "Natural fiber nonwoven reinforced cement composites as sustainable materials for building envelopes." *Construction and Building Materials* 115: 230-239. doi:10.1016/j.conbuildmat.2016.04.044.

Dasong, D., and F. Mizi. 2010. "Characteristic and performance of elementary hemp fibre." *Materials Sciences and Applications* 1: 336-342. doi:10.4236/msa.2010.16049.

Deraman, M., S. Zakaria, M. Husin, R. Aziz, R. Ramli, A. Mokhtar, M. N. M. Yusof, and M. H. Sahri. 1999. "X-ray diffraction studies on fiber of oil palm empty fruit bunch and rubberwood for medium-density fiberboard." *Journal of Materials Science Letters* (Springer) 18 (3): 249-253.

Deraman, M., S. Zakaria, and J. A. Murshidi. 2001. "Estimation of crystallinity and crystallite size of cellulose in benzylated fibres of oil palm empty fruit bunches by x-ray diffraction." *Japanese Journal of Applied Physics* 40 (1(5A)): 3311-3314.

Dharkal, H. N., Z. Y. Zhang, and M. O. W. Richardson. 2006. "Effect of water absorption on the mechanical properties of hemp fibre reinforced unsaturated polyester composites." *Composites Science and Technology* 67: 1674-1683. doi:10.1016/j.comscitech.2006.06.019.

Faizi, M. K., A. B. Shahriman, M. S. A. Majid, B. M. T. Shamsul, A. S. M. Nawawi, I. Zunaidi, Y. G. Ng, Z. M. Razlan, and W. K. Wan. 2018. "The effect of multiple surface treatments on oil palm empty fruit bunch (OPEFB) fibre structure." *IOP Conference Series: Materials Science and Engineering.* doi:10.1088/1757-899X/429/1/012005.

Fortea-Verdejo, M., E. Bumbaris, C. Burgstaller, A. Bismarck, and K. Lee. 2017. "Plant fibre-reinforced polymers: where do we stand in terms of tensile properties?" *International Materials Reviews* 62 (8): 441-464. doi:10.1080/09506608.2016.1271089.

Goud, G., and R. N. Rao. 2013. "Combined effect of alkali and silane treatments on tensile and impact properties of roystonea regia natural fiber reinforced epoxy composites." *Applied Polymer Composites* 1 (3): 187-196.

Hestiawan, H., Jamasri, and Kusmono. 2016. "A preliminary study: Influence of alkali treatment on physical and mechanical properties of Agel leaf fiber (Corypha gebanga)." *Applied Mechanics and Materials* 842: 61-66. doi:10.4028/www.scientific.net/AMM.842.61.

Ismail, S., and Z. Yaacob. 2011. "Properties of laterite bricks reinforced with oil palm empty fruit bunch fibres." *Pertanika Journal of Science and Technology* (Universiti Putra Malaysia Press) 19 (1): 22-43.

Izani, M. N., M. T. Paridah, U. M. K. Anwar, M. M. Nor, and P. S. H'ng. 2013. "Effects of fiber treatment on morphology, tensile and gravimetric analysis of oil palm empty fruit bunches fibers." *Composites Part B: Engineering* 45 (1): 1251-1257. doi:10.1016/j.compositesb.2012.07.027.

663 Kabir, M. M., K. Lau, T. Wang, and F. Cardona. 2012. "Chemical treatments on plant-based natural fibre
664 reinforced polymer composites: An overview." *Composites: Part B* 43: 2883-2892.
665 doi:10.1016/j.compositesb.2012.04.053.

666 Kuthi, F. A. A., K. H. Badri, and A. M. Azman. 2015. "X-ray diffraction patterns of oil palm empty fruit
667 bunch fibers with varying crystallinity." *Advanced Materials Research* 1087: 321-328.
668 doi:10.4028/www.scientific.net/AMR.1087.321.

669 Machaka, M., H. Basha , H. A. Chakra, and A. Elkordi. 2014. "Alkali treatment of fan palm natural fibers
670 for use in fiber reinforced concrete." *European Scientific Journal* 10 (12): 186-195.

671 Malenab, R. A. J., J. P. S. Ngo, and M. A. B. Promentilla. 2017. "Chemical treatment of waste abaca for
672 natural fiber-reinforced geopolymer composite." *Materials* 10 (579): 1-19.
673 doi:10.3390/ma10060579.

674 Masniroszaime, M. Z., A. W. Mohammad, H. Shuhaida, A. F. Nurul, and H. H. Nur. 2018. "Synergistic
675 effects on process parameters to enhance enzymatic hydrolysis of alkaline oil palm fronds."
676 *Industrial Crops and Products* 112: 617-626. doi:10.1016/j.indcrop.2018.06.037.

677 Meheddene, M., B. Hisham, A. Hadi, and E. Adel. 2014. "Alkali treatment of fan palm natural fibres for
678 use in fibre reinforced concrete." *European Scientific Journal* 10 (12): 186-194.

679 Modenbach, A. A., and S. E. Nokes. 2014. "Effects of sodium hydroxide pretreatment on structural
680 components of biomass." *Transactions of the ASABE* 57 (4): 1187-1198.
681 doi:10.13031/trans.57.10046.

682 Momoh, E. O., and A. I. Osofero. 2019. "Behaviour of oil palm broom fibres (OPBF) reinforced concrete."
683 *Construction and Building Materials* 221: 745-761. doi:10.1016/j.conbuildmat.2019.06.118.

684 Momoh, E. O., and A. I. Osofero. 2020. "Recent developments in the application of oil palm fibres in
685 cement composites." *Frontiers of Structural and Civil Engineering*.
686 https://doi.org/10.1007/s11709-019-0576-9.

687 Momoh, E. O., and B. I. O. Dahunsi. 2017. "Suitability of oil-palm-broom-fibres as reinforcement for
688 laterite-based roof tiles." *International Journal of Software & Hardware Research in Engineering*
689 5 (4): 27-35.

690 Muñoz, E., and J. A. García-Manrique. 2015. "Water absorption behaviour and Its effect on the mechanical
691 properties of flax fibre reinforced bioepoxy composites." *International Journal of Polymer Science*
692 2015. doi:10.1155/2015/390275.

693 Mydin, M. A. O., N. Mohamad, A. A. A. Samad, I. Johari, and M. A. C. Munaaim. 2018. "Durability
694 performance of foamed concrete strengthened with chemical treated (NaOH) coconut fibers." *AIP*
695 *Conference Proceedings, vol. 2016, no. 1, p. 020109. AIP Publishing.* doi:10.1063/1.5055511 .

696 Nishiyamo, Y., and T. Okano. 1998. "Morphological changes of ramie fiber during mercerization." *Journal*
697 *of Wood Science* 44 (4): 310-313. doi:10.1007/BF00581312.

698 Nogata, F., and H. Takahashi. 1995. "Intelligent functionally graded material: Bamboo."
699 *Composites Engineering* 5(7): 743-751.

Osoka, E. C., and O. D. Onukwuli. 2015. "Optimum conditions for mercerization of oil palm empty bunch fibres." *International Journal of Innovative Research in Computer Science and Technology (IJIRCST)* 3 (4): 50-56.

Oushabi, A., F. O. Hassani, Y. Abboud, S. Sair, O. Tanane, and A. El-Bouari. 2018. "Improvement of the interface bonding between date palm fibers and polymeric matrices using alkali-silane treatments." *International Journal of Industrial Chemistry* 9: 335-343.

Ozerkan, N. G., B. Ahsan, S. Mansour, and S. R. Iyengar. 2013. "Mechanical performance and durability of treated palm fiber reinforced mortars." *International Journal of Sustainable Built Environment* 2 (2): 131-142. doi:10.1016/j.ijsbe.2014.04.002.

Pacheco-Torgal, F., and S. Jalali. 2010. "Cementitious building materials reinforced with vegetable fibres: A review." *Construction and Building Materials* 25 (2): 575-581. doi:10.1016/j.conbuildmat.2010.07.024.

Pandiarajan, P., M. Kathiresan, and T. Sornakumar. 2018. "Preparation of nanofiber particles from the leaf of Aristida hystrix and its characterization." *Journal of Natural Fibres* 16 (6): 886-897. doi:10.1080/15440478.2018.1441089.

Pangsang, N., U. Rattanapan, A. Thanapimmetha, P. Srinopphakhun, C. Liu, X. Zhao, F. Bai, and C. Sakdaronnarong. 2019. "Chemical-free fractionation of palm empty fruit bunch and palm fiber by hot-compressed water technique for ethanol production." *Energy Reports* 5: 337-348. doi:doi.org/10.1016/j.egyr.2019.02.008.

Ramamoorthy, S. K., M. Skrifvars, and M. Rissanen. 2015. "Effect of alkali and silane surface treatments on regenerated cellulose fibre type (Lyocell) intended for composites." *Cellulose* 22 (1): 637-654. doi:10.1007/s10570-014-0526-6.

Rambo, M. K. D., and M. Márcia, C. Ferreira. 2015. "Determination of cellulose crystallinity of banana residues using near infrared spectroscopy and multivariate analysis." *Journal of Brazillian Chemical Society* 26 (7): 1491-1499. doi:10.5935/0103-5053.20150118.

Ratner, B. D., and A. S. Hoffman. 2013. "Physicochemical surface modification of materials used in medicine." In *Biomaterials Science (Third Edition)*, 256-276. Elsevier. doi:10.1016/B978-0-08-087780-8.00027-9.

Santos, E. B. C., C. G. Moreno, J. J. P. Barros, D. A. de Moura, F. F. de-Carvalho, A. Ries, R. M. R. Wellen, and L. B. Da Silva. 2018. "Effect of alkaline and hot water treatments on the structure and morphology of piassava fibers." *Materials Research* 21 (2).

Segal, L., J. J. Creely, A. E. Martin, and C. M. Conrad. 1959. "An empirical method for estimating the degree of crystallinity of native cellulose using the x-ray diffractometer." *Textile Research Journal* 786-794.

Sellami, A., M. Merzoud, and S. Amziane. 2013. "Improvement of mechanical properties of green concrete by treatment of the vegetals fibers." *Construction and Building Materials* 47: 1117-1124. doi:10.1016/j.conbuildmat.2013.05.073.

737 Shah, D. U. 2013. "Developing plant fibre composites for structural applications by optimising composite
738 parameters: a critical review." *Journal of Materials Science* 48 (18): 6083-6107.
739 doi:10.1007/s10853-013-7458-7.

740 Souza, N. F., J. A. Pinheiro, A. I. S. Brígida, J. P. S. Morais, M. M. S. Filho, and R. M. de Freitas. 2016.
741 "Fibrous residues of palm oil as a source of green chemical building blocks." *Industrial Crops and*
742 *Products* 94: 480-489. doi:10.1016/j.indcrop.2016.09.012.

743 Sreekala, M. S., J. George, M. G. Kumaran, and S. Thomas. 2001. "Water-sorption kinetics in oil palm
744 fibers." *Journal of Polymer Science: Part B: Polymer Physics* (John Wiley & Sons Inc.) 39: 1215-
745 1223.

746 Sreekala, M. S., M. G. Kumaran, and S. Thomas. 1997. "Oil Palm Fibers: morphology, chemical
747 Composition, surface modification, and mechanical properties." *Journal of Applied Polymer*
748 *Science* 66 (5): 821-835. doi:10.1002/(SICI)1097-4628(19971031)66.

749 Sreekala, M. S., and S. Thomas. 2002. "Effect of fibre surface modification on water-sorption
750 characteristics of oil palm fibres." *Composites Science and Technology* 63: 861-869.
751 doi:10.1016/S0266-3538(02)00270-1.

752 Symington, M. C., O. S. David-West, W. M. Banks, R. A. Pethrick, and J. Thomason. 2008. "The effect of
753 alkalisation on the mechanical properties of natural fibres." *13th European Conference on*
754 *Composite Materials (EECM 13).*

755 Tagne, N. R. S., E. Njeugna, M. Fogue, J.-Y. Drean, A. Nzeukou, and D. Fokwa. 2014. "Study of water
756 absorption in Raffia vinifera fibres from Bandjoun, Cameroon." *The Scientific World Journal* 2014
757 1-11. doi:10.1155/2014/912380

758 Terán-Hilares, R., A. L. Reséndiz, R. T. Martínez, S. S. Silva, and J. C. Santos. 2016. "Successive
759 pretreatment and enzymatic saccharification of sugarcane bagasse in a packed bed flow-through
760 column reactor aiming to support biorefineries." *Bioresource Technology* 203: 42-49.
761 doi:10.1016/j.biortech.2015.12.026.

762 Van de Weyenberg, I., T. C. Truong, B. Vangrimde, and I. Verpoest. 2006. "Improving the properties of
763 UD flax fibre reinforced composites by applying an alkaline fibre treatment." *Composites Part A:*
764 *applied science and manufacturing* 37: 1368-1376. doi:10.1016/j.compositesa.2005.08.016.

765 Wang, B., S. Panigrahi, L. Tabil, and W. Crerar. 2007. "Pre-treatment of flax fibers for use in rotationally
766 molded biocomposites." *Journal of Reinforced Plastics and Composites* 26 (5): 447-463.
767 doi:10.1177/0731684406072526.

768 Wang, W., M. Sain, and P. A. Cooper. 2006. "Study of moisture absorption in natural fibre composites."
769 *Compos Sci Technol* 66: 379-386.

770 Wei, J., and C. Meyer. 2014. "Improving degradation resistance of sisal fiber in concrete through fiber
771 surface treatment." *Applied Surface Science* 289: 511-523. doi:10.1016/j.apsusc.2013.11.024.

772 Zannen, S., L. Ghali, M. T. Halimi, and M. B. Hssen. 2014. "Effect of chemical extraction on
773 physicochemical and mechanical properties of doum palm fibres." *Advances in Materials Physics*
774 *and Chemistry* 4: 2013-216. doi:10.4236/ampc.2014.410024.

775 Zhou, Y., M. Fan, and C. Lihui. 2016. "Interface and bonding mechanisms of plant fibre composites: An
776 overview." *Composites Part B* 101: 31-45. doi:10.1016/j.compositesb.2016.06.0551359-8368.

777

778

779

780

781

782

783

784

785

786

787

788

789

790

791

792

793

794

795

796

797

798

799

800

801

802

Tables

Table 1: Water absorption of treated and untreated OPBF at room temperature

OPBF sample type	Saturation water absorption w_s (%)	Initial slope of plot (k)	Diffusion coefficient D, x 10^{-3} (mm^2/min)
untreated	53.39	3.0586	1.847
2 hours Hot-water	58.13	6.0111	3.827
48 hours 2%NaOH	73.17	10.5861	7.872
48 hours 4%NaOH	86.96	13.4701	4.442
48 hours 6%NaOH	58.62	11.5750	9.775
48 hours 10%NaOH	52.63	10.191	13.81
24hours 1%Silane	42.85	1.4168	0.49
24hours 3%Silane	48.28	4.9187	3.205
48hours 1%Silane	48.89	4.7560	4.476
48hours 3%Silane	55.26	2.8686	1.01

Table 2: Results of X-Ray diffraction test

Sample	Peak height of crystalline region (I_{002}) / 2θ angle	Height of Amorphous region (I_{am}) / 2θ angle	Crystallinity Index (CI) (%)
Untreated	11224.38 / 21.35^0	8957.93 / 16.68^0	20.2
Alkalisation	13096.49 / 21.96^0	9299.60 / 18.41^0	29.0
Silane treated	12901.57 / 21.62^0	9655.24 / 18.12^0	25.2
Hot-water treated	12704.38 / 21.49^0	10048.99 / 17.83^0	21.0

Physico-mechanical Properties of Treated Oil Palm Broom Fibres for Cementitious Composites

Emmanuel Owoichoechi Momoh[1] Adelaja Israel Osofero[2*] Oleksandr Menshykov[3]
School of Engineering, University of Aberdeen, Kings College, Aberdeen, United Kingdom[1,2,3]
r01eom18@abdn.ac.uk[1], aiosofero@abdn.ac.uk[2], o.menshykov@abdn.ac.uk [3]

FIGURES

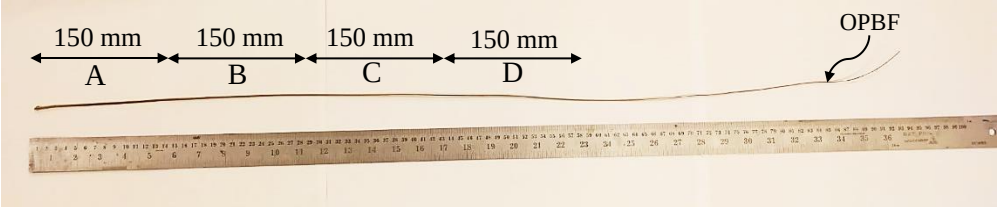

Fig. 1. Illustration of the 4-Categories of OPBF

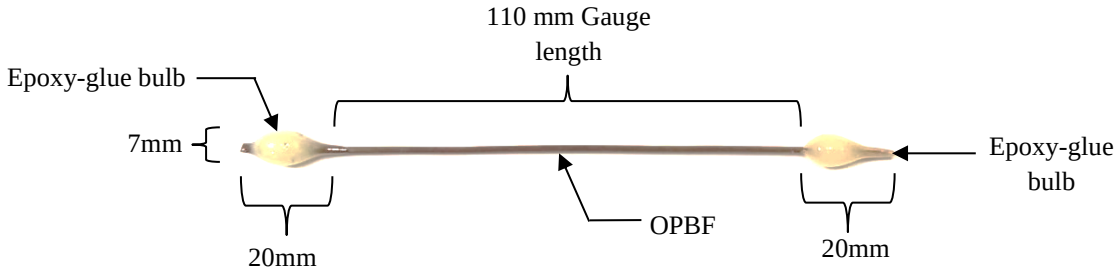

Fig. 2. An OPBF prepared for tensile testing showing dimension details

826

827

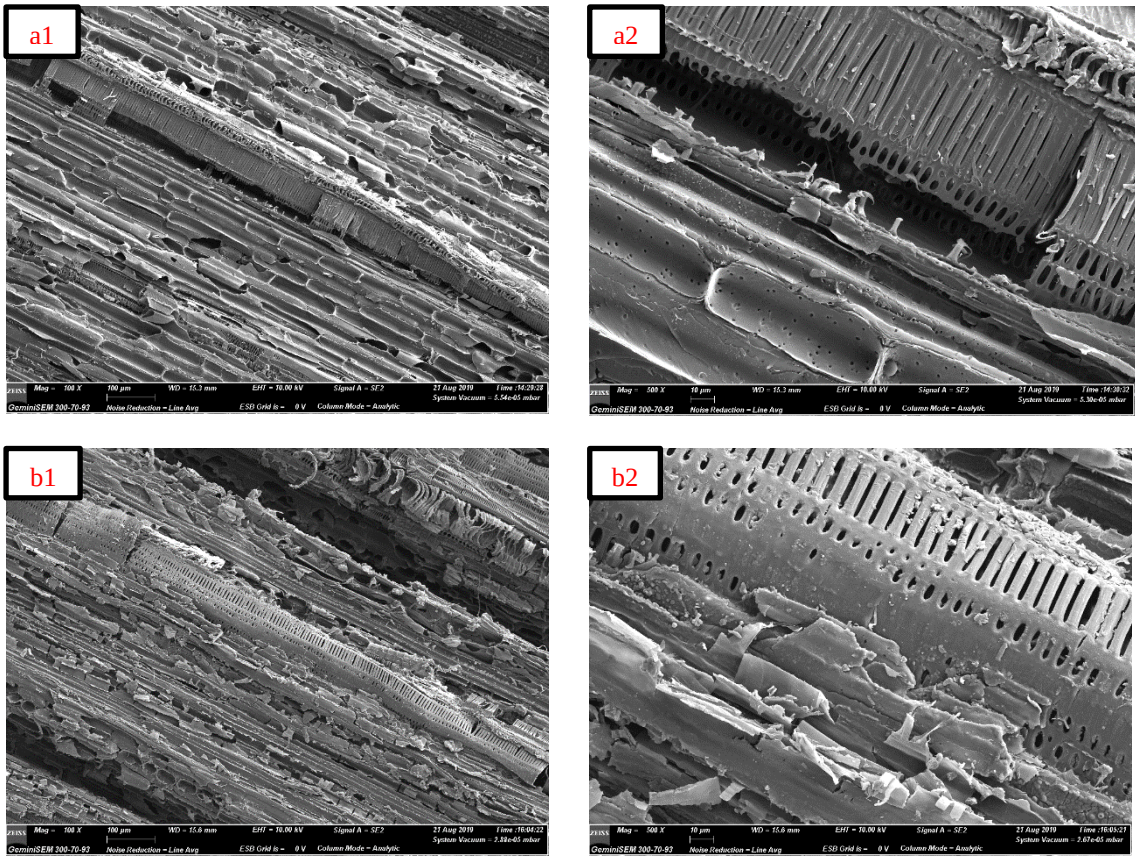

Fig. 3. SEM images of OPBF longitudinal sections
(a1) Untreated OPBF 100x **(a2)** Untreated OPBF 500x
(b1) Alkali-treated OPBF-6% NaOH at 48 hours 100x **(b2)** Alkali-treated OPBF-6% NaOH at 48 hours 500x

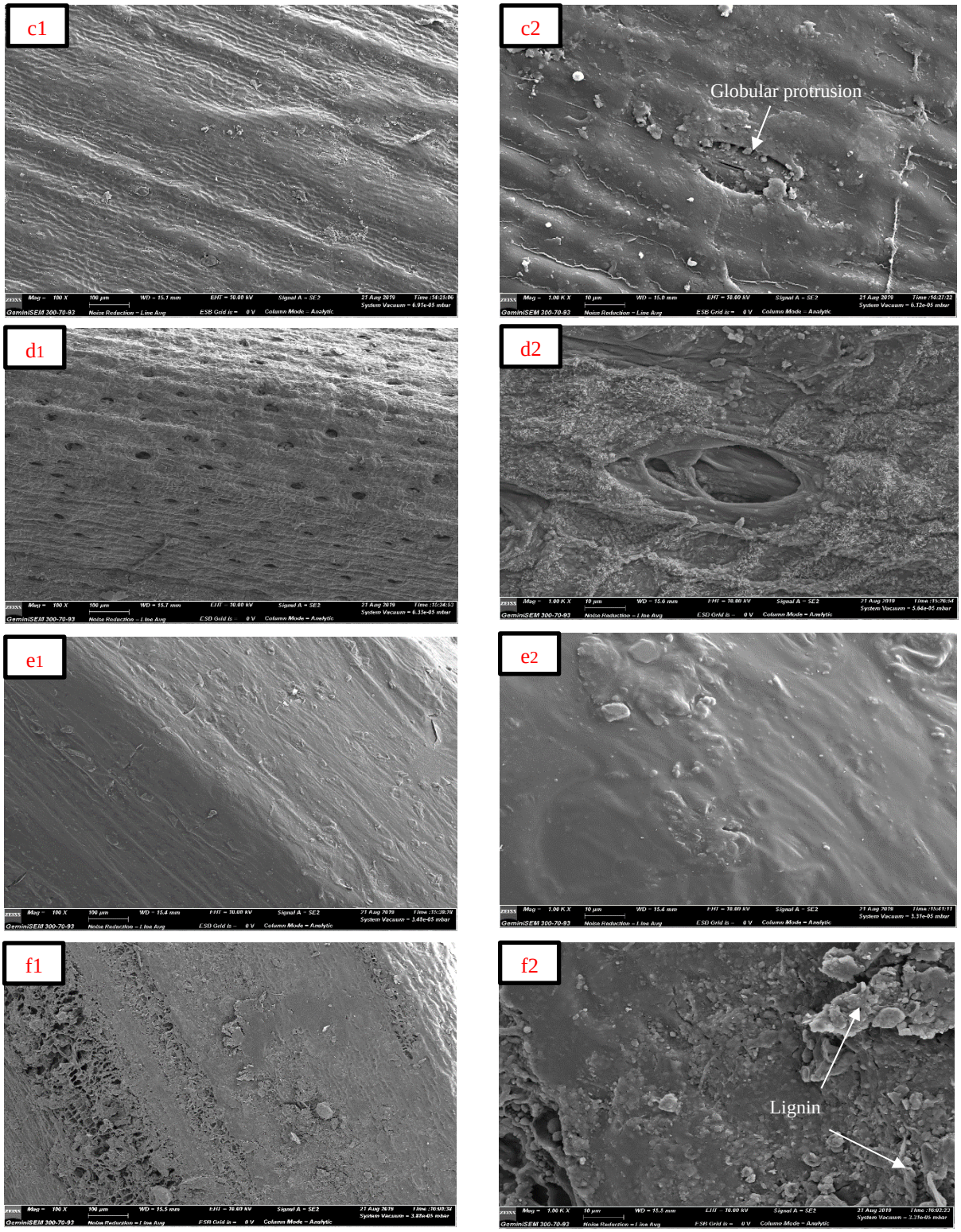

Fig. 4. SEM images of OPBF surface **(c1)** Untreated OPBF 100x **(c2)** Untreated OPBF 1000x **(d1)** Alkali-treated OPBF-6% NaOH at 48 hours 100x **(d2)** Alkali-treated OPBF-6% NaOH at 48 hours 1000x **(e1)** Silane-treated OPBF – 3% silane at 48 hours 100x **(e2)** Silane-treated OPBF – 3% silane at 48 hours 1000x
(f1) Hot water treatment-2 hours 100x **(f2)** Hot water treatment-2 hours 1000x

828

829

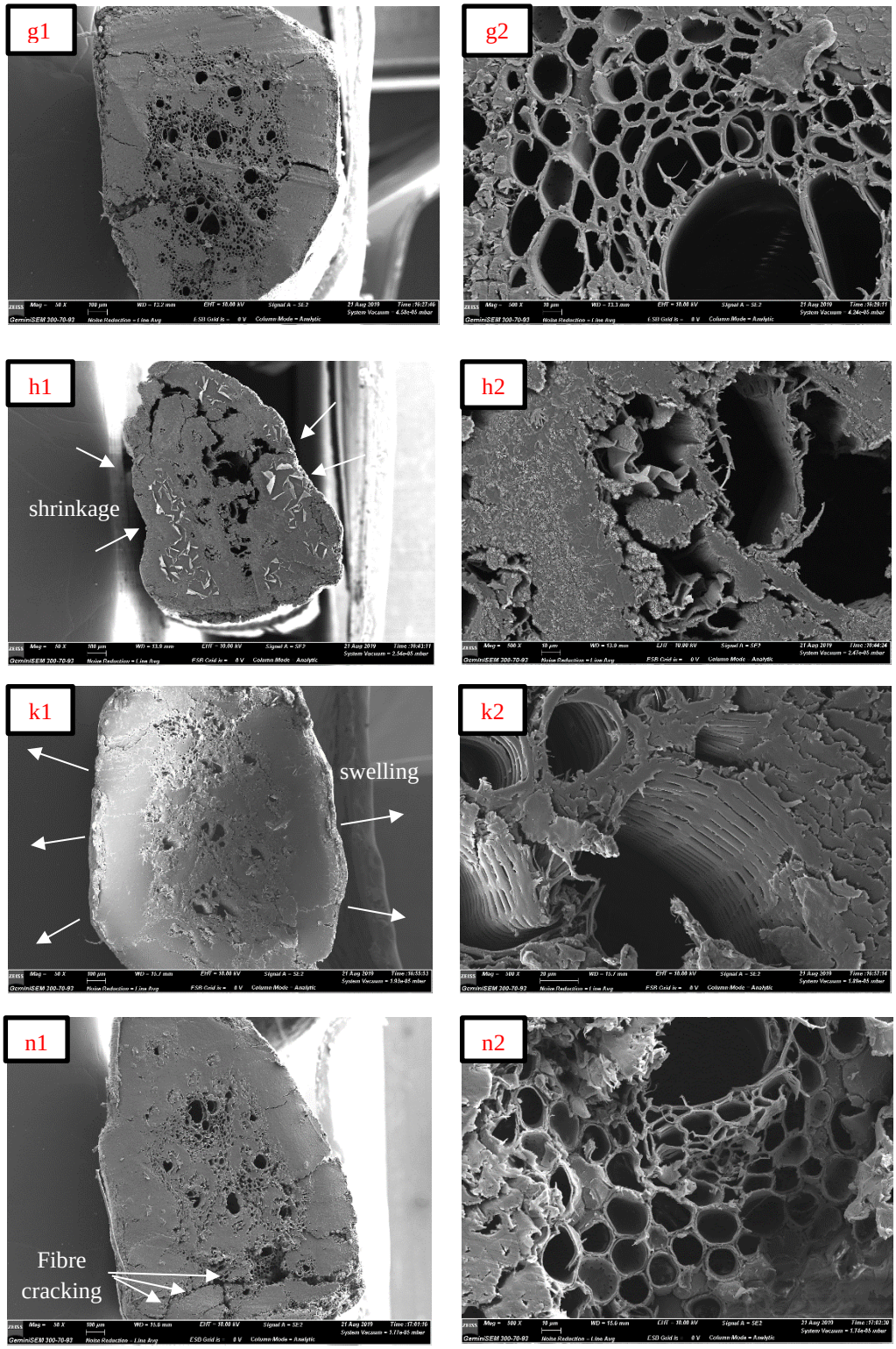

Fig. 5. SEM images of OPBF cross-sections
(g1) Untreated OPBF 50x **(g2)** Untreated OPBF 500x
(h1) Alkali-treated OPBF-6% NaOH at 48 hours 50x **(h2)** Alkali-treated OPBF-6% NaOH at 48 hours 500x
(k1) Silane-treated OPBF – 3% silane at 48 hours 50x **(k2)** Silane-treated OPBF – 3% silane at 48 hours 500x
(n1) Hot-water treated OPBF-2 hours 100x **(n2)** Hot-water treated OPBF-2 hours 500x

Fig. 6. Change in colour of water: before start of treatment (left) after hot-water/alkali-treatment (middle) and silane treatment (right) of OPBF

830

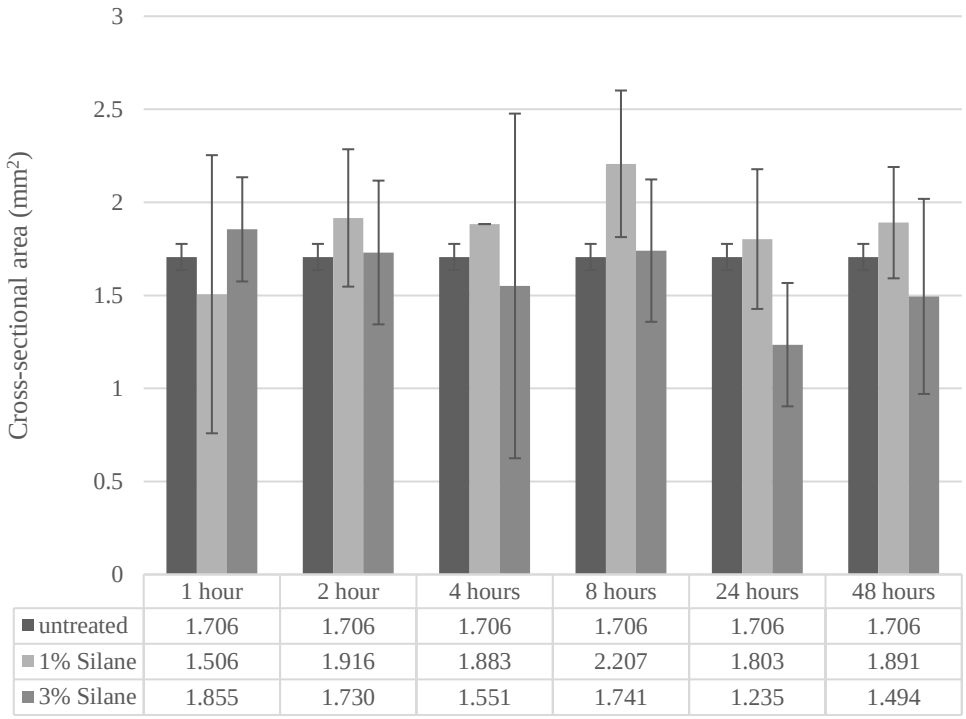

	1 hour	2 hour	4 hours	8 hours	24 hours	48 hours
untreated	1.706	1.706	1.706	1.706	1.706	1.706
1% Silane	1.506	1.916	1.883	2.207	1.803	1.891
3% Silane	1.855	1.730	1.551	1.741	1.235	1.494

Fig. 7. Cross-sectional areas after *Silane-treatment of OPBF* for different time durations

831

832

833

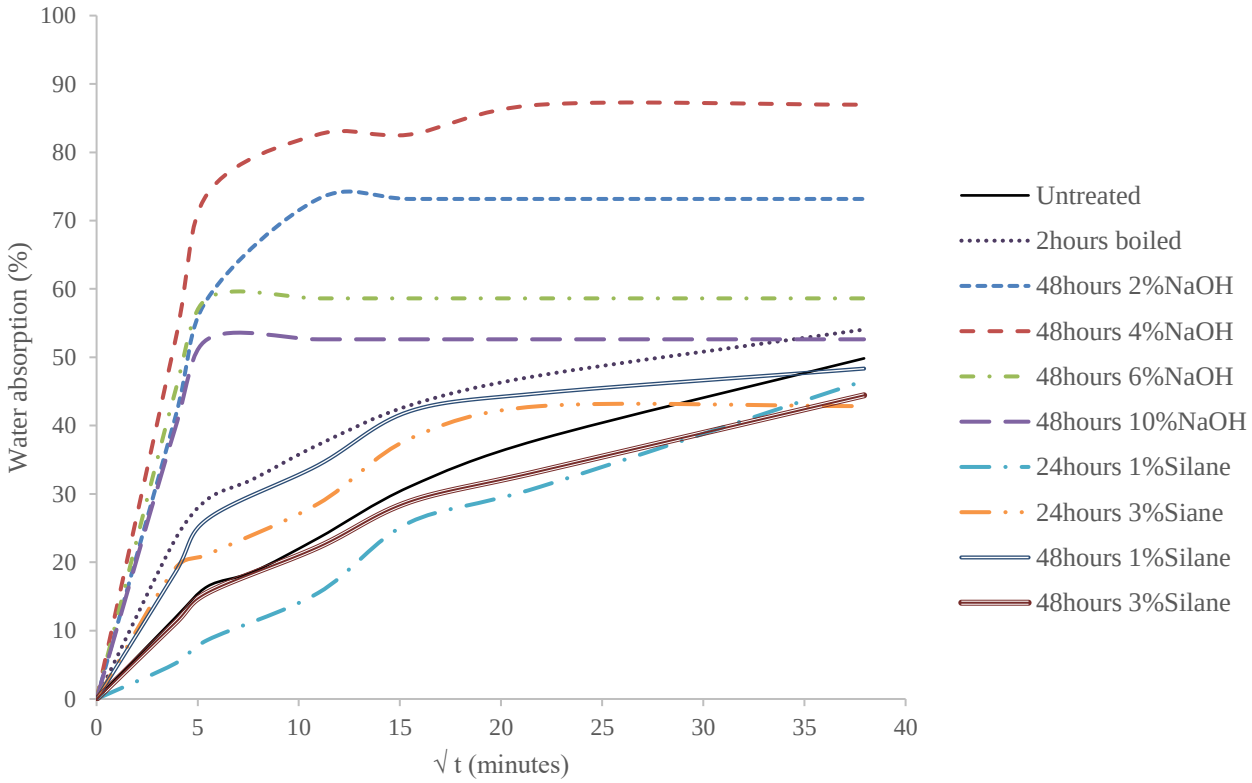

Fig. 8. Water absorption of untreated and treated OPBF

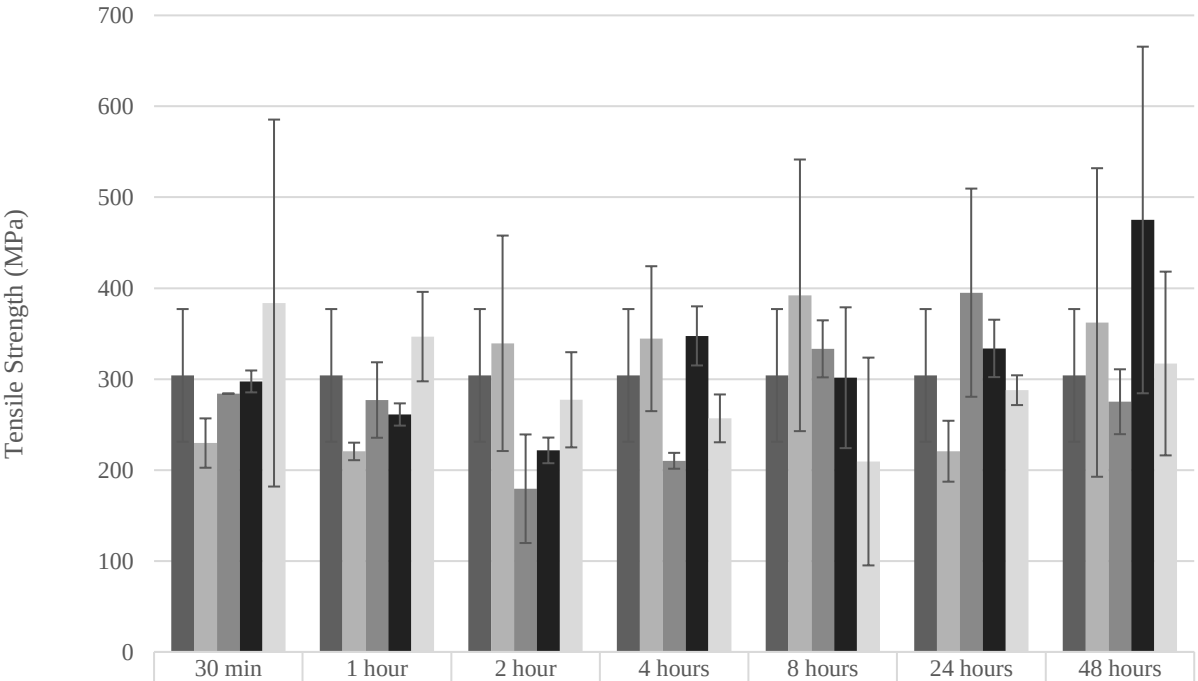

	30 min	1 hour	2 hour	4 hours	8 hours	24 hours	48 hours
Untreated	304.06	304.06	304.06	304.06	304.06	304.06	304.06
2% NaOH	229.69	220.49	339.39	344.45	392.15	220.71	362.28
4% NaOH	284.02	277.02	179.46	210.19	333.30	395.05	275.13
6% NaOH	297.46	261.10	221.61	347.53	301.55	333.78	475.01
10% NaOH	383.65	346.76	277.27	256.85	209.40	287.83	317.15

Fig. 9. Tensile strength of OPBF subjected to *NaOH treatment* at various concentrations and treatment durations

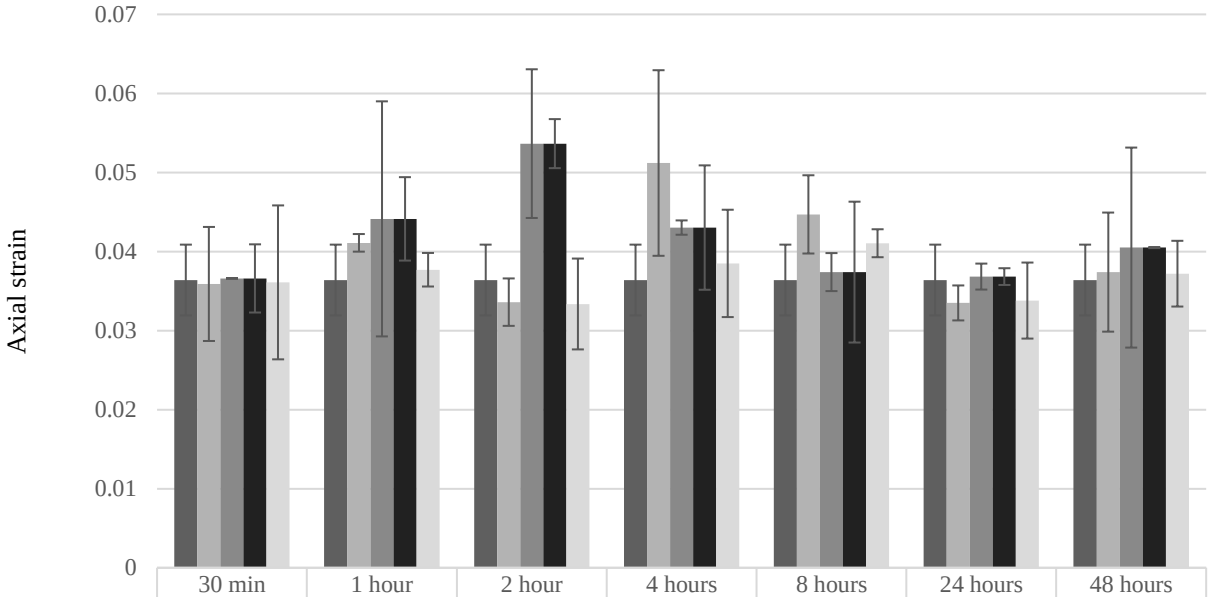

	30 min	1 hour	2 hour	4 hours	8 hours	24 hours	48 hours
untreated	0.0364	0.0364	0.0364	0.0364	0.0364	0.0364	0.0364
2% NaOH	0.0359	0.0411	0.0336	0.0512	0.0447	0.0335	0.0374
4% NaOH	0.0366	0.0441	0.0537	0.0430	0.0374	0.0368	0.0405
6% NaOH	0.0366	0.0441	0.0537	0.0430	0.0374	0.0368	0.0405
10% NaOH	0.0361	0.0377	0.0334	0.0385	0.0411	0.0338	0.0372

Fig. 10. Strain at failure of OPBF subjected to *NaOH-treatment* at various concentrations and treatment durations

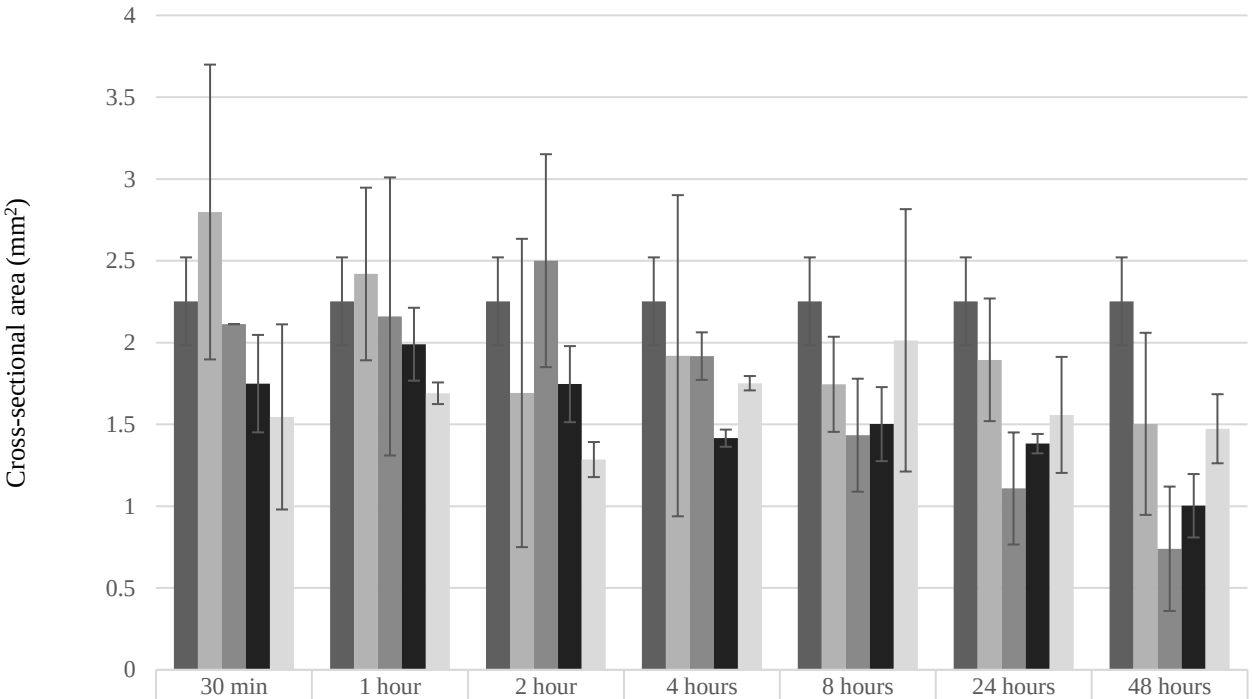

	30 min	1 hour	2 hour	4 hours	8 hours	24 hours	48 hours
untreated	2.252	2.252	2.252	2.252	2.252	2.252	2.252
2% NaOH	2.798	2.420	1.692	1.920	1.745	1.895	1.504
4% NaOH	2.113	2.160	2.501	1.918	1.434	1.109	0.740
6% NaOH	1.750	1.990	1.746	1.416	1.502	1.383	1.003
10% NaOH	1.546	1.691	1.285	1.752	2.014	1.558	1.474

Fig. 11. Cross-sectional areas after *NaOH-treatment of* OPBF for different time durations

863

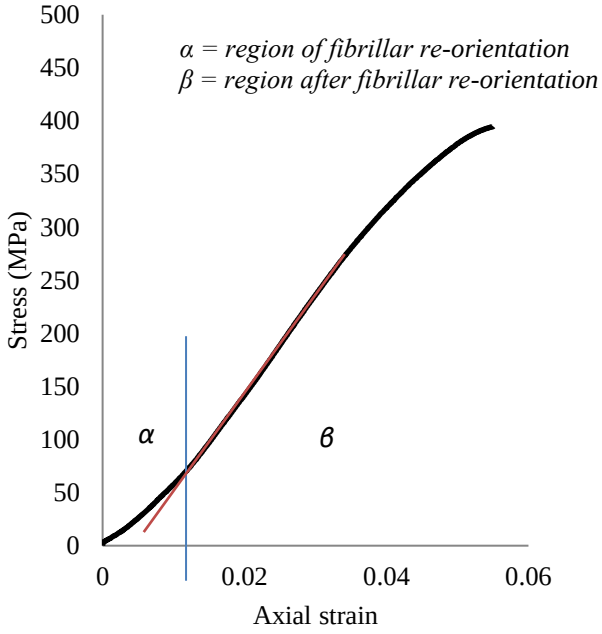

Fig. 12. Typical stress-strain curve for OPBF from tensile strength test

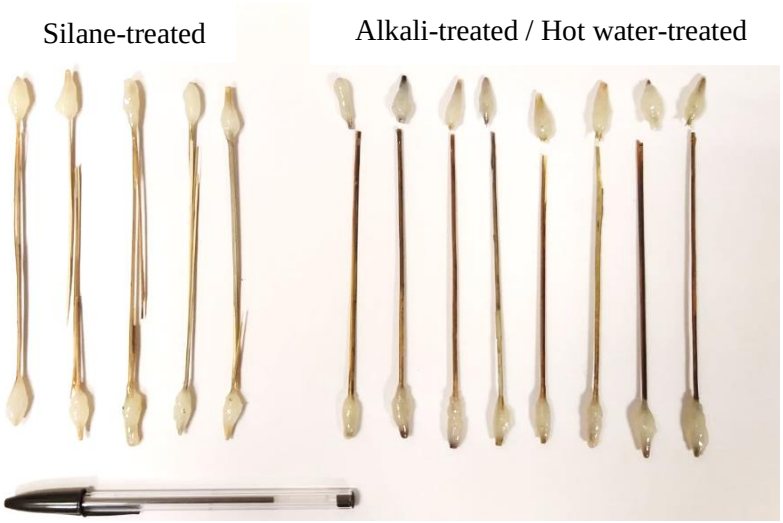

Fig. 13. Distinct failure modes of treated OPBF samples

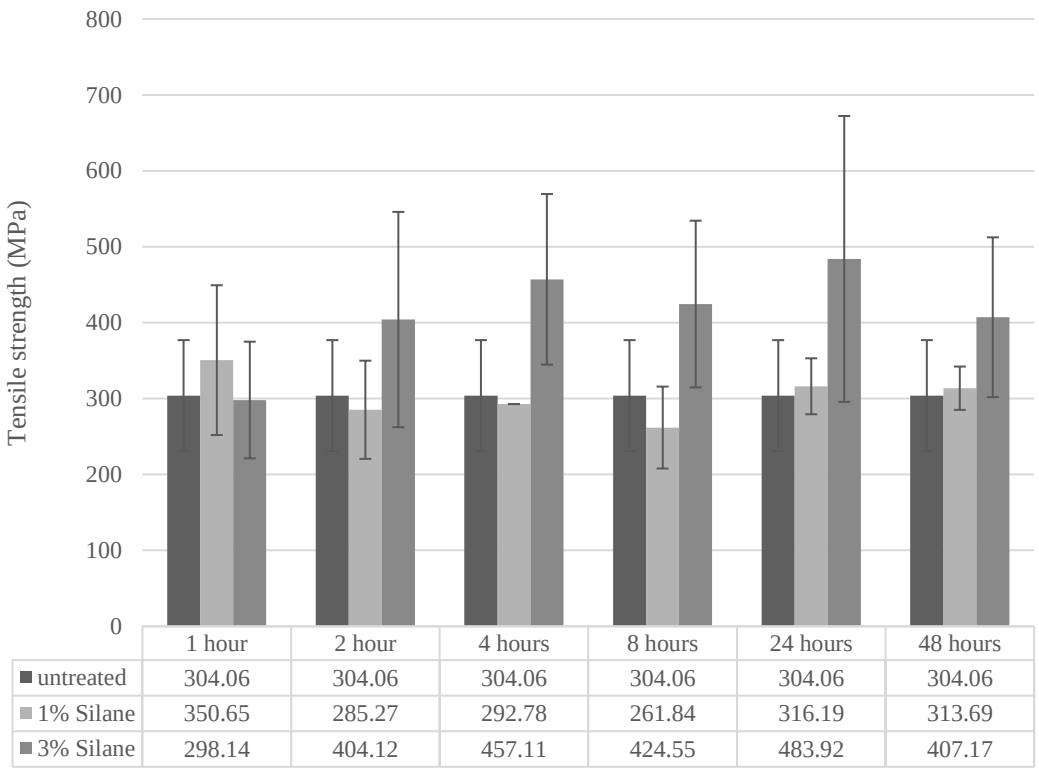

	1 hour	2 hour	4 hours	8 hours	24 hours	48 hours
untreated	304.06	304.06	304.06	304.06	304.06	304.06
1% Silane	350.65	285.27	292.78	261.84	316.19	313.69
3% Silane	298.14	404.12	457.11	424.55	483.92	407.17

Fig. 14. Tensile strength of OPBF subjected to *Silane treatment* at various concentrations and treatment durations

876

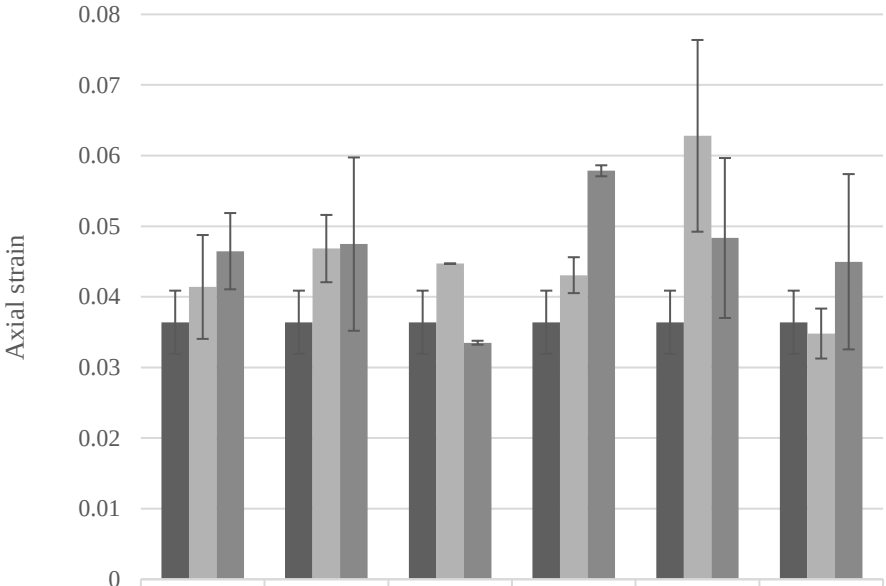

	1 hour	2 hour	4 hours	8 hours	24 hours	48 hours
untreated	0.0364	0.0364	0.0364	0.0364	0.0364	0.0364
1% Silane	0.0414	0.0468	0.0447	0.0431	0.0628	0.0348
3% Silane	0.0465	0.0475	0.0335	0.0579	0.0483	0.0450

Fig. 15. Strain at failure of OPBF subjected to *Silane-treatment* at various concentrations and treatment durations

877

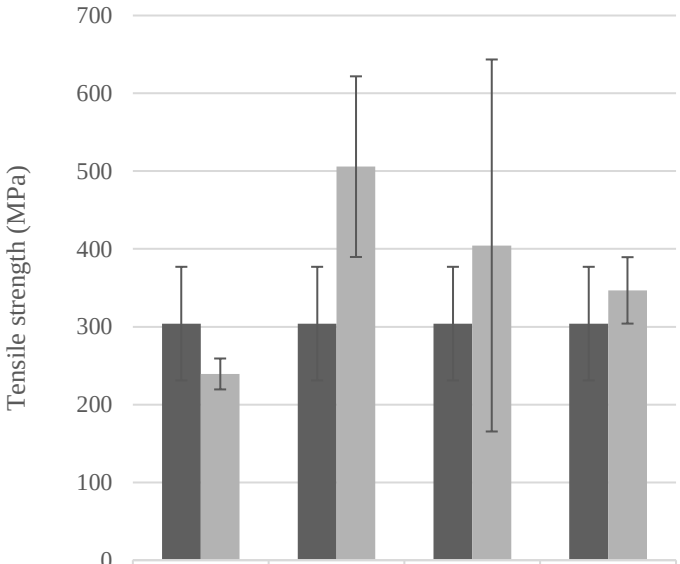

	15 min	30 min	1 hour	2 hour
untreated	304.06	304.06	304.06	304.06
Boiling	239.33	505.77	404.46	346.73

Fig. 16. Tensile strength of OPBF subjected to *Hot-water treatment* for different time durations

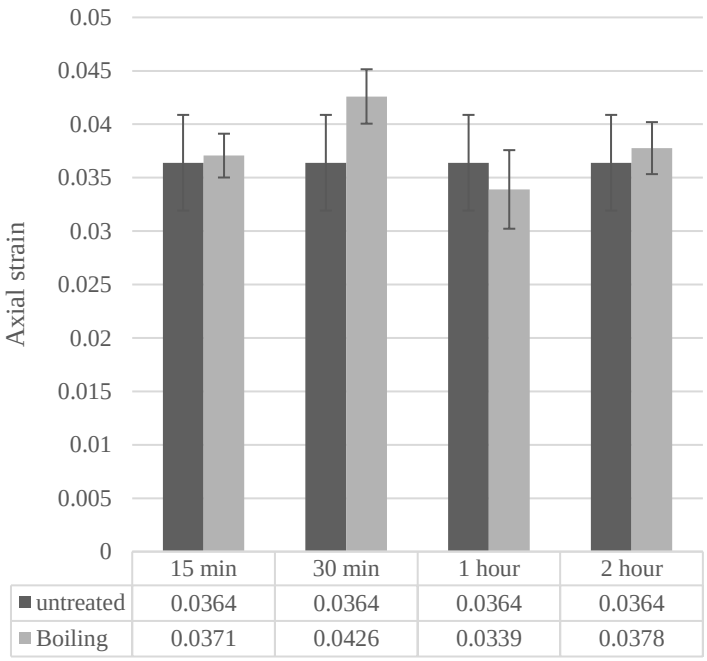

Fig. 17. Strain at failure of OPBF subjected to *Hot-water treatment* for different time durations

878

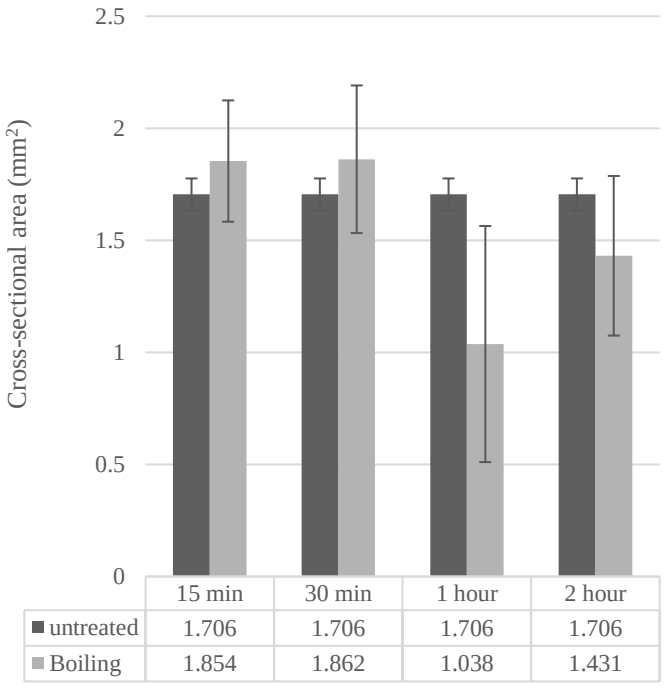

Fig. 18. Cross-sectional areas after *Hot water-treatment of* OPBF for different time durations

879

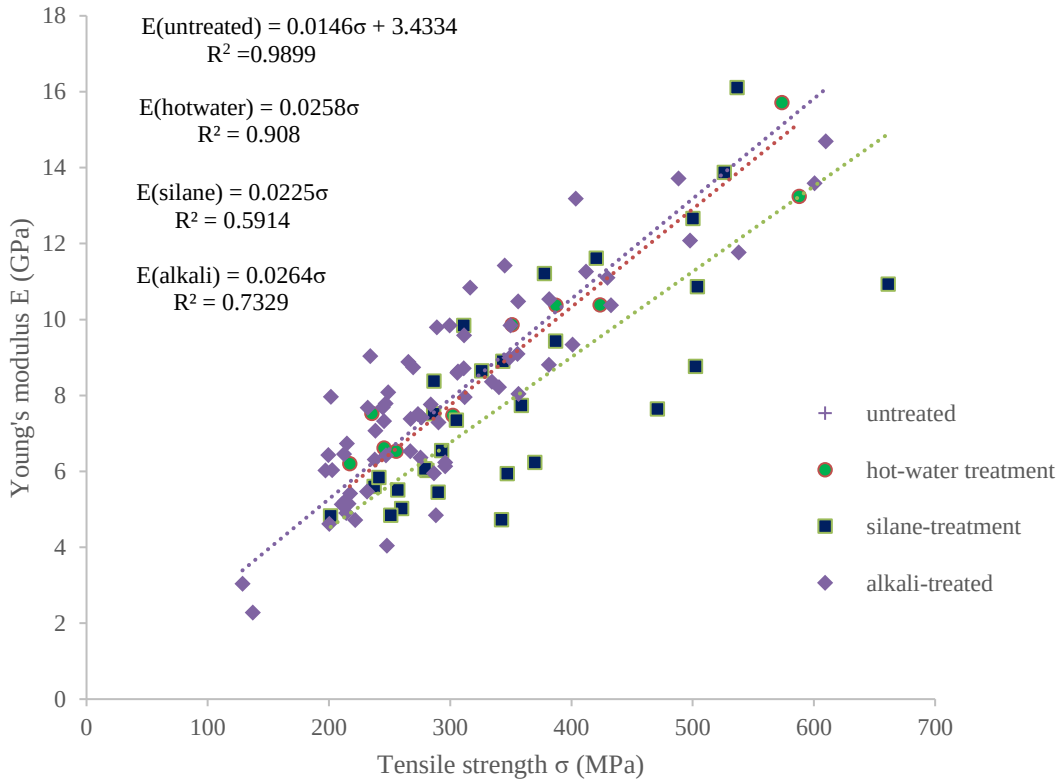

Fig. 19. Tensile Strength (σ) versus Young's modulus (E) relationship for treated OPBF

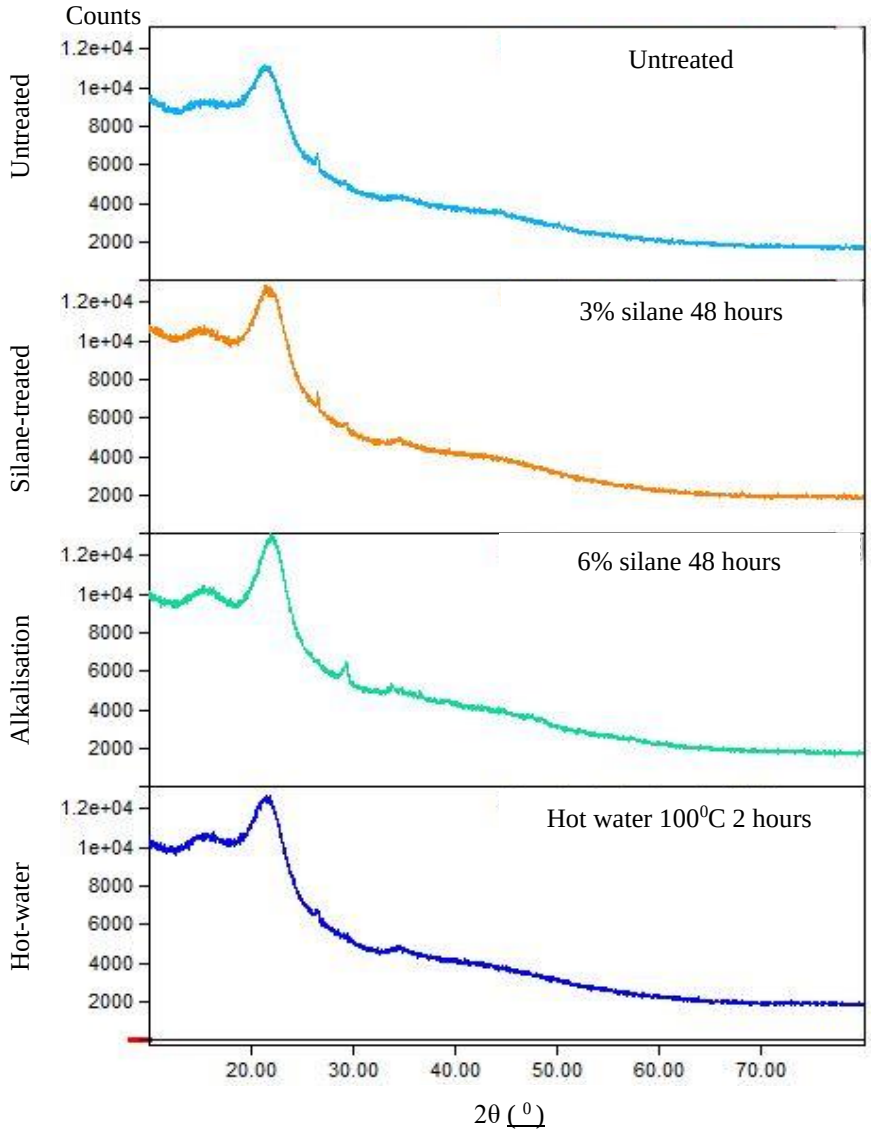

Fig. 20. X-ray diffraction profiles of untreated and treated OPBF